

The techno-economics of biocarbon production processes under Norwegian conditions

Maciej Olszewski, Rajesh S. Kempegowda, Øyvind Skreiberg, Liang Wang, and Terese Løvås

Energy Fuels, **Just Accepted Manuscript** • DOI: 10.1021/acs.energyfuels.6b03441 • Publication Date (Web): 11 Nov 2017

Downloaded from <http://pubs.acs.org> on November 13, 2017

Just Accepted

“Just Accepted” manuscripts have been peer-reviewed and accepted for publication. They are posted online prior to technical editing, formatting for publication and author proofing. The American Chemical Society provides “Just Accepted” as a free service to the research community to expedite the dissemination of scientific material as soon as possible after acceptance. “Just Accepted” manuscripts appear in full in PDF format accompanied by an HTML abstract. “Just Accepted” manuscripts have been fully peer reviewed, but should not be considered the official version of record. They are accessible to all readers and citable by the Digital Object Identifier (DOI®). “Just Accepted” is an optional service offered to authors. Therefore, the “Just Accepted” Web site may not include all articles that will be published in the journal. After a manuscript is technically edited and formatted, it will be removed from the “Just Accepted” Web site and published as an ASAP article. Note that technical editing may introduce minor changes to the manuscript text and/or graphics which could affect content, and all legal disclaimers and ethical guidelines that apply to the journal pertain. ACS cannot be held responsible for errors or consequences arising from the use of information contained in these “Just Accepted” manuscripts.



The techno-economics of biocarbon production processes under Norwegian conditions

Maciej Olszewski^{a,c}, Rajesh S. Kempegowda^b, Øyvind Skreiberg^b, Liang Wang^b, Terese Løvås^a

^aDepartment of Energy & Process Engineering, NTNU, Trondheim, Norway

^bSINTEF Energy Research, Trondheim, Norway

^cAGH University of Science and Technology, Faculty of Energy and Fuels, Krakow, Poland

Corresponding author: rajesh.kempegowda@sintef.no

Abstract

This work deals with techno-economic analysis studies in the context of production of various grade biocarbon for utilization as reducing agents in metallurgical industries. A detailed process design was developed for wood handling, debarking, chipping, drying, carbonization, and combined heat and power production using Aspen Plus for 10 ton per day (TPD) biocarbon output. A Fortran based user defined function was developed for the carbonization process by considering pressure, temperature and particle size effects using a Box – Behnken approach. The empirical correlation indicates a strong influence of temperature as well as a significant influence of pressure and particle size on the biocarbon yield and its fixed carbon content. Fixed carbon content increases with temperature, pressure and particle size. Mass and energy balance results from Aspen Plus provided necessary results for cost parametrization considering three influencing parameters; temperature, pressure and plant scale on the equipment costs, operating expenses and production cost of biocarbon. Four scenarios are compared i.e. logwood supply, woodchips supply, co-production of biooil and replacing the carbonization agent from nitrogen to air. The results indicate that logwood supply is more economical than supplying woodchips to the plant gate. Economic benefits in terms of cost is ~5% (at 1 bar and 450-500°C, 55-60 TPD) and ~4% (at 10 bar, 450-500°C, 55-60 TPD). Co-production of biooil decreased the production cost of biocarbon (\$/GJ) by 40-44% (at 1 bar, 450-500°C, 40-60 TPD) and 30-36% (at 10 bar, 450-500°C, 40-60 TPD), respectively. Finally, the economic return based on IRR suggests that highest IRR is achieved for scenario C, where biooil is a co-product, it is due

1
2
3 28 to high market price of woody tar at 500 \$/ton. Transportation of forest biomass (logwood)
4
5 29 from 20 to 220 km increased the cost of logwood from 4.75 \$/GJ to 7.15 \$/GJ, which is
6
7 30 significant in terms of operating cost.
8
9
10 31

11 **Keywords:** Biocarbon/Charcoal, Carbonization, Process design and simulation,
12
13 parametric cost modelling
14
15
16 34

18 35 **1. Introduction**

20 36 Norwegian metal production industries are facing challenges with respect to CO₂ emissions.
21
22 37 According to Statistics Norway ¹, metallurgical industries use large quantities of pit coal
23
24 38 briquettes, about 541990 tons per year, and coal coke and semi-coke, around 353818 tons
25
26 39 per year, as reducing agent during production. As well, wood charcoal is used in these
27
28 40 sectors in the amount of 26000 tons annually. Under Norwegian conditions, 100% of the
29
30 41 charcoal is imported. The major source of bioenergy in Norway is forest biomass ² and the
31
32 42 main kinds of trees are spruce, pine, birch and alder ³. In that perspective, Norway has
33
34 43 potential to utilize forest woody biomass as an attractive alternative feedstock for the
35
36 44 production of high value energy carriers such as charcoal/biocarbon. Charcoal/biocarbon is
37
38 45 produced in a thermochemical conversion process that operates under inert atmosphere or
39
40 46 starved oxygen condition called carbonization ^{4, 5}. Traditional carbonization processes are
41
42 47 heavily criticized due to the low yield of charcoal and direct emissions generated by these
43
44 48 industries ⁶. Charcoal is considered to be an international commodity; charcoal production
45
46 49 in these traditional production processes demands a long residence time and gives a low
47
48 50 charcoal yield ^{4, 7}. According to worldwide charcoal utilization, 50 million tons of charcoal
49
50 51 is consumed for various industrial uses, for example as reducing agent ⁸, co-firing and as a
51
52 52 domestic cooking fuel in developing countries ⁶. With an assumption of 15% average
53
54
55
56
57
58
59
60

1
2
3 53 charcoal yield on dry wood basis, there is a consumption of 1 billion m³ of woody biomass.
4
5 54 Hence, there is a demand for more sustainable charcoal production processes to be applied
6
7 55 in the industrial sector. As well in the European region, there is large consumption of coal,
8
9 56 coke and other fossil derived synthetic carbon as reductants in the metal production
10
11 57 industries. This is causing a wide range of damaging effects such as emission intensity raise
12
13 58 and health hazards. To tackle the low yield charcoal production processes and improve the
14
15 59 economic viability, self-sustainable production of charcoal under Norwegian conditions is
16
17 60 highly relevant. Carbonization processes can be classified based on the temperature regimes
18
19 61 of operation in the pyrolysis process as a low temperature carbonization (torrefaction) and
20
21 62 high temperature carbonization. This depends on the use of upgraded biomass of different
22
23 63 grades for the purpose of reducing agent in metal production furnaces or co-firing in
24
25 64 furnaces or boilers. Biocarbon product quality is normally assessed based on the fixed
26
27 65 carbon content as the main quality index criteria in several metallurgical industries.
28
29 66 Aluminum production requires very high fixed carbon content, above 95%, whereas SiMn
30
31 67 and FeMn around 95%, Si and FeSi above 70% and SiC above 80%. In that perspective,
32
33 68 carbonization process operating conditions, as peak temperature in the carbonization
34
35 69 process, have an influential effect on reaction paths and biocarbon properties^{9, 10}. However
36
37 70 increasing the temperature reduces the yield of charcoal. This demands a process that can
38
39 71 mimic the natural process occurring under the earth based on an elevated pressure, which
40
41 72 plays a significant role in improving the yield of charcoal and fixed carbon. Studies on the
42
43 73 influence of elevated pressure dates back to 1853, started by Violette et al.¹¹. Later, there is
44
45 74 decades of experience from University of Hawaii, and also in collaboration with Norwegian
46
47 75 researchers, by Antal and coworkers on the influence of elevated pressure in a flash type
48
49 76 carbonization reactor for various feedstocks^{9, 12-14}. Recently, a few works from Australia in
50
51 77 the area of improved charcoal production using an auto-thermal reactor at atmospheric
52
53
54
55
56
57
58
59
60

1
2
3 78 conditions have been reported ^{15, 16}. Other important parameters that govern the process are
4
5 79 vapor residence time and heating rates, influencing the charcoal yield and fixed carbon
6
7 80 content ^{9, 17}. Depending on the process operating conditions and process reactor the quality
8
9
10 81 of biocarbon in terms of fixed carbon content, reactivity, porosity and surface area will be
11
12 82 influenced. Based on these properties, biocarbon can be utilized for cooking, residential
13
14 83 heating, peak load boilers, adsorbent, soil conditioning and metallurgical production. In this
15
16 84 context, a detailed techno-economic evaluation of carbonization processes based on plant-
17
18 85 gate analysis is carried out under Norwegian conditions. This work deals with techno-
19
20 86 economic studies in the context of production of various grade biocarbon as reducing agents
21
22 87 and for co-firing in the metallurgical industries. The plant gate analysis involves process
23
24 88 system analysis using Aspen Plus with user defined functions development using Fortran
25
26 89 expressions for the wood handling zone consisting of debarking, chipping, drying,
27
28 90 carbonization process and combined heat and power (CHP) production. This study also
29
30 91 investigates the influence of process conditions such as carbonization temperature, pressure
31
32 92 and particle size on the overall biocarbon yield through semi-empirical methods. The case
33
34 93 design is developed based on the principles of an integrated process system analysis
35
36 94 approach. A novel simplified multifunctional regression model has been proposed to predict
37
38 95 the product yields as a function of the carbonization process parameters temperature,
39
40 96 pressure and particle size. The study also integrates a heat and power system coupled to the
41
42 97 carbonization process to produce electricity and provide heat to external customers, e.g.
43
44 98 district heat production. A techno-economic value chain is designed for the supply of
45
46 99 biomass from the Norwegian forest, for example spruce, as a potential feedstock.
47
48
49
50
51
52 100

53 54 101 **2. Process plant design and approach**

55
56
57
58
59
60

1
2
3 102 Figure 1 shows the process flow diagram for the biomass carbonization plant. Main process
4
5 103 steps are i) feedstock handling consisting of stem wood storage, debarking, chipping and
6
7 104 screening, chips drying, ii) carbonization process and iii) combined heat and power
8
9 105 production. Process plant design is carried out in the commercial software Aspen Plus using
10
11 106 user defined Fortran programming. The commercial process simulation software is based on
12
13 107 the basic engineering relations (mass and energy balance, phase equilibrium and reaction
14
15 108 kinetics). This allows simulating process behaviors including chemical reactions. It is
16
17 109 possible to simulate one block element or the complete integrated system for different
18
19 110 process configurations. In this work, the Peng – Robinson equation of state was used for
20
21 111 properties determination. The advantage of using a cubic form is that it has capability to
22
23 112 handle non ideal behavior for hydrocarbons¹⁸. Details of the process models developed in
24
25 113 each process zone are presented below.
26
27
28
29
30
31

114

115 **2.1 Feedstocks characteristics**

116 Norwegian spruce biomass is considered as the feedstock. Fuel characterization such as
117 proximate analysis, ultimate analysis and heating values are shown in Table 1 for spruce
118 stem wood, spruce woodchips, spruce bark and spruce forest residues.

119

120 **2.2 Process modelling and simulation**

121 **Logwood handling system modelling in Aspen Plus:** Logwood harvested from the forestry
122 is transported via trucks to the carbonization plant. Logwood harvested will have a cut length
123 of 3 m. The diameter of the logwood can vary from 0.15 m to 0.5 m (Norwegian Institute of
124 Bioeconomy Research). Logwood handling system consists of debarking to remove the bark,
125 chipping, screening and drying as shown in Figure 2. Details of the sub-process models are
126 depicted in the following subsections.

1
2
3 127 **Debarking process:** Traditionally, bark separation from the stem wood was usually carried
4
5 128 out for pulping processes. The advantage of bark separation in the pulping process is to
6
7 129 reduce the cooking chemical consumption as well as to avoid contamination due to ash rich
8
9 130 compounds (silica and calcium compounds, dirt) ¹⁹. Similarly, bark separation is also
10
11 131 relevant in the biocarbon production for metallurgical industry. The amount of bark on the
12
13 132 stem wood varies according to tree species, for spruce 8-15%, for birch 7-15% and for pine
14
15 133 10-17% ²⁰. According to standard EN14961-2, production of Class A1 pellets from bark for
16
17 134 energy purpose is not suitable due to the high ash content in the bark. In a drum debarker, the
18
19 135 volumetric loading is in the range of 25-35% with a drum speed around 4-7 rpm. In our
20
21 136 estimation we used industrial data (length: 18 m and 5 m diameter) and a residence time in
22
23 137 the debarking process of around 40 mins (Jan 2016). In the Aspen Plus system model, a
24
25 138 simple splitter model is used with user defined expressions. Specific electricity consumption
26
27 139 P [kW] for the debarker (DE) was calculated as shown in equation 1, where X_{DE} – electricity
28
29 140 consumption for static load [kW], S_{DE} – static load [kg/h] and M_{LOG} – logwood mass flow
30
31 141 rate [kg/h]. In the model power requirement for debarker (X_{DE}) is 34.5 kW and the static
32
33 142 load (S_{DE}) is 85000 kg/h.

34
35
36
37
38
39 143
$$P_{DE} = \frac{X_{DE}}{S_{DE}} \cdot M_{LOG} \quad (1)$$

1
2
3 144 **Chipping and screening:** Quality specifications and classes selected in the biocarbon process
4
5 145 value chain is based on the European standards (e.g. EN 14961-1), this includes all solid
6
7 146 biofuels and it is probably targeted for industries, even though it is meant for all groups. The
8
9 147 particle sizes are classified according to standard EN 15149-1. Typically, metallurgical
10
11 148 industries require an ash content below 3%²¹. The chipper model is based on industrial scale
12
13 149 data, implemented as a Fortran expression in the model. Specific power consumption P [kW]
14
15 150 for the chipper (CH) is based on mass flow rate into the chipper according to equation 2.

$$18 \quad 19 \quad 20 \quad 21 \quad 22 \quad 23 \quad 24 \quad 25 \quad 26 \quad 27 \quad 28 \quad 29 \quad 30 \quad 31 \quad 32 \quad 33 \quad 34 \quad 35 \quad 36 \quad 37 \quad 38 \quad 39 \quad 40 \quad 41 \quad 42 \quad 43 \quad 44 \quad 45 \quad 46 \quad 47 \quad 48 \quad 49 \quad 50 \quad 51 \quad 52 \quad 53 \quad 54 \quad 55 \quad 56 \quad 57 \quad 58 \quad 59 \quad 60$$

$$151 \quad P_{CH} = \frac{X_{CH}}{S_{CH}} \cdot M_{IN-CHIP} \quad (2)$$

152 where X_{CH} – electricity consumption for static load [kW], S_{CH} – static load [kg/h] and $M_{IN-CHIP}$ – mass flow rate into the chipper [kg/h]. A power consumption X_{CH} of 522.5 kW and a corresponding static load S_{CH} of 36000 kg/h are used as a model parameters. The screening model is based on the Aspen Plus built in model. Weight fractions data are gathered from Laitila et al.²². Weight fractions for the drum and disc chipper used in the model are shown in Table 2.

158 **Chips drying:** The belt dryer model use air as a drying medium. Heat is supplied by flue gas and LP steam from the CHP unit. Drying rate is calculated based on a drying curve for woodchips, experimental data is gathered from Johansson et al.²³, and the normalized drying rate $v(\alpha)$ according to equation 3 is implemented in Aspen Plus, and are shown in Figure 3 and also included as supplementary data in Appendix D.

$$163 \quad v(\alpha) = \frac{\text{current drying rate}}{\text{drying rate 1st drying period}} \quad \alpha = \frac{Z - Z_{eq}}{Z_{cr} - Z_{eq}} \quad (3)$$

164 where α – normalized moisture content, Z – current moisture content on dry basis [kg/kg],
165 Z_{cr} – Critical moisture content on dry basis (0.831 kg/kg), Z_{eq} – equilibrium moisture
166 content on dry basis (0.01 kg/kg)²⁴ depends on the relative humidity and temperature of the
167 drying medium, air. The drying rate is expressed in kg/(kg/s). For our drying conditions,
168 reaching a moisture content of 10% is a reasonable assumption, and the normalised drying

1
2
3 169 rate have in this work been applied until achieving this moisture content. Air goes first
4
5 170 through heat exchangers (HE) where heat from the recycled air is recovered, next the air is
6
7 171 preheated by flue gas, and the last heat exchanger is used when flue gas is not sufficient to
8
9 172 provide all the heat needed and then low-pressure steam is used. Hot air is split into two
10
11 173 streams, that are directed to the second and third stages. After that they are mixed and
12
13 174 directed to the first stage as shown in Figure 4. The heat demand is dependent on the
14
15 175 moisture content in the feedstock.
16
17

18 176 **Carbonization process modelling:** A schematic is shown in Figure 5. The heart of the
19
20 177 process design is the carbonization reactor. The sub-model for the carbonization reactor is
21
22 178 modelled through development of an empirical multifunctional regression model using
23
24 179 experimental yields from several literature sources^{4, 9, 10, 25}. The yields data are included as
25
26 180 supplementary data in Appendix C. The model for the carbonization/pyrolysis is based on an
27
28 181 user defined yield calculator using Fortran expressions. Heat to the reactor is supplied by
29
30 182 flue gas. The pressure in the pressurized pyrolysis is provided by compressed nitrogen or air,
31
32 183 where the air in this work is considered inert with respect to the pyrolysis products
33
34 184 prediction. Pyrogas and biooil are burnt in the combustor to produce heat for the pyrolysis
35
36 185 process and for CHP production. The main product is biocarbon.
37
38
39

40 186 Pyrolysis modeling to predict products:
41
42
43
44
45
46
47
48
49
50
51
52
53
54
55
56
57
58
59
60

1
2
3 187 Pyrolysis modeling to predict products is done in accordance with
4
5 188 Neves et al.²⁶. The model allows prediction of the carbon, hydrogen and oxygen (CHO)
6
7 189 composition of produced biocarbon [kg/kg dry ash free biocarbon] based on empirical
8
9 190 equations, which are correlated to temperature (T) in °C:

$$10 \quad 191 \quad Y_{C,BC} = 0.93 - 0.92 \cdot \exp(-0.42 \cdot 10^{-2} \cdot T), R^2 = 0.65 \quad (4)$$

$$11 \quad 192 \quad Y_{H,BC} = -0.41 \cdot 10^{-2} + 0.10 \cdot \exp(-0.24 \cdot 10^{-2} \cdot T), R^2 = 0.75 \quad (5)$$

$$12 \quad 193 \quad Y_{O,BC} = 0.07 + 0.85 \cdot \exp(-0.48 \cdot 10^{-2} \cdot T), R^2 = 0.56 \quad (6)$$

13
14
15
16
17
18 194 These equations are reasonable and validated for woody biomass by Neves et al.²⁶.
19
20 195 Woodchips produced in the chipper below 3.15 mm becomes dust (sawdust) and above 45
21
22 196 mm is reintroduced into the chipper. The model was developed by gathering literature data
23
24 197 for the biocarbon yield.

25
26
27 198 Biocarbon yield by statistical design:

28
29
30 199 Biocarbon yield ($Y_{biocarbon}$) was introduced by a Box – Behnken approach. This approach is
31
32 200 rotatable and requires three levels for each factor. The main purpose is to optimize the
33
34 201 response surface, which is impacted by the process condition^{27, 28}. This approach can be
35
36 202 expressed by equation 7.

$$37 \quad 38 \quad y = \beta_0 + \sum_{i=1}^k \beta_i x_i + \sum_{i=1}^k \beta_{ii} x_i^2 + \sum_{i=1}^{k-1} \sum_{j=2}^k \beta_{ij} x_i x_j + \varepsilon \quad (7)$$

39
40
41 203 where x_1, x_2, \dots, x_k are the input variables which influence the response of y , $\beta_0, \beta_i, \beta_{ii}$ ($i = 1,$
42
43 204 $2, \dots, k$), β_{ij} ($i = 1, 2, \dots, k; j = 1, 2, \dots, k$) are unknown parameters and ε is a random error.
44
45 205 The β coefficients are obtained by the least squares method²⁷. The developed biocarbon
46
47 206 yield [kg/kg dry biomass] function ($Y_{biocarbon}$) is shown in equation 8.

$$48 \quad 49 \quad 50 \quad 51 \quad 207 \quad Y_{biocarbon} = 126.3 - 0.3406 \cdot T - 4.5 \cdot p + 4.13 \cdot d + 0.00031 \cdot T^2 + 0.19 \cdot p^2 - 0.204 \cdot d^2 \quad (8)$$

$$52 \quad 53 \quad 54 \quad 208 \quad + 0.0050 \cdot T \cdot p - 0.00971 \cdot T \cdot d + 2.29 \cdot p \cdot d, \quad R^2 = 0.90$$

55
56 209 where T is temperature in °C, p is pressure in bar and d is particle diameter in mm.

Gas yields [kg/kg dry ash free biomass] are based on empirical equations which are functions of temperature (T in °C, in the range 350 – 1000 °C)²⁶. Main gas compounds in the pyrolysis gas are usually H₂O, H₂, CH₄, C₂H₄, CO and CO₂.

$$Y_{H_2} = 1.145 \cdot (1 - \exp(-0.11 \cdot 10^{-2} \cdot T))^{9.384}, \quad R^2 = 0.94 \quad (9)$$

$$Y_{CO} = Y_{H_2} \cdot \frac{1}{3 \cdot 10^{-4} + \frac{0.0429}{1 + (T/632)^{-7.23}}}, \quad R^2 = 0.73 \quad (10)$$

$$Y_{CH_4} = -2.18 \cdot 10^{-4} + 0.146 \cdot Y_{CO}, \quad R^2 = 0.88 \quad (11)$$

Additionally an equation for the pyrolysis gas LHV in MJ/kg was used to calculate the energy balance of the pyrolysis process (T in °C)²⁶.

$$LHV_{gas} = -6.23 + 2.47 \cdot 10^{-2} \cdot T, \quad R^2 = 0.78, \quad 300-900^\circ\text{C} \quad (12)$$

The Neves et al.²⁶ correlations indicate that there is a weak relationship between the elemental composition of tar and pyrolysis temperature. The recommended correlations²⁶ for the tar elemental composition [kg/kg dry tar] is shown in equations 13 to 15.

$$Y_{C,tar} = 1.14 \cdot Y_{C,biomass} \quad (13)$$

$$Y_{H,tar} = 1.13 \cdot Y_{H,biomass} \quad (14)$$

$$Y_{O,tar} = 0.80 \cdot Y_{O,biomass} \quad (15)$$

where $Y_{i,biomass}$ is the biomass elemental composition [kg/kg, dry ash free basis].

The products carbon dioxide (CO₂), ethylene (C₂H₄) and biooil (organics and water) are calculated based on (C, H, O) balances and energy balance based on LHV by solving a set of equations in the spreadsheet solver. The reader should understand that by implementing this pyrolysis products modelling approach the pressure influence only adheres directly to the biocarbon yield and indirectly to the yields of biooil and gas, however, not directly to their composition. I.e. this means that to satisfy conservation of mass, elements and energy, the unknowns in the gas composition must be adjusted accordingly. As C₂H₄ is a minor species compared to the other remaining unknown carbon containing gas species, i.e. CO₂, the CO₂ concentration must then be adjusted to satisfy the conservation laws. Even if this

1
2
3 235 results in an incorrect gas composition as a function of pressure, this do not really matter in
4
5 236 this work, as it is the energy content and the elemental composition of the gas that matters,
6
7 237 and not the species composition.
8

9
10 238 The model assumes that biooil consists of two model compounds, acetic acid (CH_3COOH)
11
12 239 and phenol ($\text{C}_6\text{H}_6\text{O}$), in addition to water. The mass ratio is assumed to be 1:1 when closing
13
14 240 the mass balance, which is reasonable assumption due to decomposition of cellulose and
15
16 241 lignin in a wider temperature range for slow pyrolysis conditions. The yield functions
17
18 242 developed in the Excel solver are reintroduced as Fortran functions in Aspen Plus. The
19
20 243 model is able to close both mass and energy balances in the temperature range of 300 to
21
22 244 500°C and in the pressure range 1-20 bar. Mass balance results for the carbonization model
23
24 245 at 500°C and varied pressure are shown in Table 3. According to the validated results, the
25
26 246 gas yields do not change very significantly for pressurized carbonization under slow
27
28 247 pyrolysis conditions²⁹.
29
30

31 32 Pyrolysis reactor sizing and scaling:

33
34 249 The concept of the pressurized reactor is based on Flash CarbonizationTM by Antal et al.^{12, 29,}
35
36 250 ³⁰. The design idea is to use 2 or 3 pressurized vessels in a swing mode (semi – continuous)
37
38 251 as shown in Figure 6(a) and (b). Woody biomass dried in the belt drier is conveyed to the
39
40 252 pyrolysis reactor and pressurized to the desired carbonization pressure by the carbonization
41
42 253 agent, nitrogen or air. Nitrogen to carbonization reactor is used based on the experimental
43
44 254 data of Lucas et al.⁴. The heat for the carbonization process is supplied by flue gas. As a
45
46 255 simplification in this work, the pyrolysis products modelling is independent of using
47
48 256 nitrogen or air as carrier gas, i.e. they are both considered inert agents. This is a justifiable
49
50 257 assumption as in the case of air the amount used is too low to support gasification of char,
51
52 258 and hence a direct influence of the air addition on the pyrolysis process and its products yield
53
54 259 can be neglected. This assumption then enables using the same biocarbon yield model
55
56
57
58
59
60

1
2
3 260 independent of the carrier gas, and the choice of the Flash Carbonization reactor then
4
5 261 becomes a generic choice.
6

7 262 **CHP:** The Aspen CHP flow sheet is presented in Figure 7. Pyrolysis volatiles (biooil) and
8
9 263 non-condensable gases are combusted in the combustor. The combustor is simulated by the
10
11 264 built-in Aspen Plus Gibbs reactor model. Hot flue gas is passing through a series of heat
12
13 265 exchangers (superheater, re-heater, evaporator and flash drum using built in Aspen Plus heat
14
15 266 exchanger models). This mimics an industrial boiler³¹, and remaining heat from the flue gas
16
17 267 is passing through the economizer and air preheater. The flue gas after the air preheater
18
19 268 supplies heat to the dryer. Part of the flue gas after the superheater is used to supply heat to
20
21 269 the pyrolysis reactor (as shown in Figure 7). After heat recovery the flue gas goes to the
22
23 270 stack. The production of steam is fixed to 700 kg/h independently from operating conditions,
24
25 271 because the amounts and quality of pyrolysis gas and biooil is varying. HP steam is produced
26
27 272 with a steam quality of 550 °C and 60 bar, and the power to steam ratio is kept constant at
28
29 273 0.18. HP steam is expanded in a series of steam turbines (high pressure, intermediate
30
31 274 pressure and low pressure) where electricity is produced. LP steam after the LP turbine is
32
33 275 used for drying and district heat production. Recycled condensed steam is mixed with the
34
35 276 make-up water and pumped to the economizer.
36
37
38
39

40 277 Details of the design specifications implemented in Aspen Plus are
41
42 278 shown in Table 4. The pressure was limited to 10 bar to avoid extreme combinations of
43
44 279 parameters according to the Box – Behnken approach.
45
46
47

48 280

49 281 **3. Biocarbon process system efficiency analysis**

50
51 282 The details of the mass and energy flows for major identified streams are supplemented as
52
53 283 respectively appendixes A and B for the 10 TPD biocarbon output base case plant. The
54
55 284 tables includes the effect of carbonization process conditions (T, P) on the mass and energy
56
57
58
59
60

1
2
3 285 flows through the system for logwood entering the plant with 40% moisture content on wet
4
5 286 basis, which is according to the PFD shown in Figure 1. Based on the mass and energy flows
6
7 287 simulation results, overall system efficiencies, that is biocarbon energy efficiency, district
8
9 288 heat (hot water) efficiency, electricity generation efficiency and overall heat utilization
10
11 289 efficiency are illustrated below. The mass and energy flows are also used in the techno-
12
13 290 economic analysis.
14
15
16
17

291

292 3.1 Biocarbon energy efficiency

293 Elevated pressure results in increased biocarbon yield and higher fixed carbon yield as
294 shown in Figure 8(a) and (b), where the fixed carbon yield [kg/kg dry ash free biomass] is
295 defined by

$$296 \quad y_{FC} = Y_{\text{biocarbon}} \cdot \frac{FC}{100-A} \quad (16)$$

297 where FC – percent fixed carbon content in the dry biocarbon on mass basis, A – percent
298 ash content in the dry biomass on mass basis and the biocarbon yield [kg/kg dry biomass], is
299 defined as

$$300 \quad Y_{\text{biocarbon}} = \frac{m_{\text{biocarbon}}}{m_{\text{biomass}}} \quad (17)$$

301 where $m_{\text{biocarbon}}$ is the mass flow rate of dry biocarbon [kg/h] and m_{biomass} is the mass
302 flow rate of dry biomass [kg/h].

303 As well, to utilize biocarbon in metal production industries, quality criteria for the biocarbon
304 product vary depending on the type of metal production industry, but generally the fixed
305 carbon content should be above 70%. This means increasing the operating temperature to
306 400 – 500 °C. The feedstock moisture content does not influence the biocarbon energy
307 efficiency, since in each case the feedstock is dried to 10% moisture content on wet basis
308 before entering the carbonization reactor, however, it influences on the additional energy
309 requirement for heating up the moisture/water vapor in the pyrolysis process. Hence, in this

1
2
3 310 work we have not studied the effect of moisture content on the carbonization process. Even
4
5 311 though the moisture content in the feedstock may have an influence on the biocarbon yield,
6
7 312 we have kept the moisture content of 10% on wet basis which is a reasonable assumption
8
9 313 based on the experimental results from Antal et al.⁷. However, increased pressure gives an
10
11 314 increased biocarbon yield while both increasing pressure and temperature also give an
12
13 315 increased fixed carbon yield. This means that there is a coupling between pressure and
14
15 316 temperature in increasing the fixed carbon yield, which is also confirmed by the literature⁴,
16
17 317 ^{9,13}. In this model the fixed carbon content is only dependent on temperature.

18
19
20
21 318 Biocarbon energy efficiency is defined as

22
23 319
$$\eta_{\text{biocarbon}} = \frac{m_{\text{biocarbon}} \cdot \text{HHV}_{\text{biocarbon}}}{m_{\text{biomass}} \cdot \text{HHV}_{\text{biomass}}} \quad (18)$$

24
25
26 320 where, m – mass flow rate [kg/h], HHV – higher heating value [MJ/kg]. Effect of operating
27
28 321 pressure and temperature on the biocarbon energy efficiency is shown in Figure 8(c). The
29
30 322 trend shows that biocarbon energy efficiency decreases as the peak temperature increases
31
32 323 from 300-500 °C, because of volatiles losses (Figure 8(a)). However, these volatiles losses
33
34 324 favors an increased fixed carbon content in the biocarbon (Figure 8(b)).

35 36 37 38 39 325 **3.2 Effect of feedstock moisture content on district heat efficiency**

40
41 326 District heat efficiency is defined as

42
43
44 327
$$\eta_{\text{DH}} = \frac{Q_{\text{DH}}}{m_{\text{biomass}} \cdot \text{HHV}_{\text{biomass}}} \quad (19)$$

45
46 328 where Q_{DH} – heat available for district heat production [MJ/h]. Moisture content has strong
47
48 329 influence on district heat efficiency (Figure 9). Increasing the pyrolysis temperature
49
50 330 improves district heat efficiency (Figure 9), which is because the production of volatiles are
51
52 331 higher and they are used as fuel. Increasing the pressure causes a slight decrease in district
53
54 332 heat efficiency because it favors secondary pyrolysis reactions and hence less tar is
55
56 333 produced. For the wood having 60% moisture, there is no district heat production for export,

all the low-pressure steam is consumed for thermal drying of the feedstock (Figure 9(c)).
Extra heat is needed and this penalty equals 8 – 9.4% of the HHV of input biomass.

336

3.3 Electricity generation efficiency

Electricity generation efficiency is defined as

$$\eta_{el} = \frac{3.6 \cdot P_{el}}{m_{biomass} \cdot HHV_{biomass}} \quad (20)$$

where P_{el} – electricity output from the turbines [kW]. Base case steam production is fixed to 700 kg/h at all operating conditions. This is due to variations in the quality and quantity of produced fuel (pyrolysis gas and biooil). At lower temperatures less fuel is produced and 700 kg/h is minimum steam load. Base case electricity produced in the steam turbine is 127.95 kW, which is according to the fixed steam load to the turbine. Total production of biocarbon is set to 10 TPD biocarbon output in the base case model. Raw feedstock mass flow rate is changing according to biocarbon yield, which is a function of temperature and pressure. Electricity consumption is calculated based on mass flow rate in each equipment. Electricity generation efficiency is shown in Figure 9(d). Electricity generation efficiency decreases with increasing temperature, which is because the yield of biocarbon decreases. However, the steam load is set to minimum level and a portion of the steam is fed to the drying zone, which is depending on the moisture content. Low-pressure steam bled from the steam turbine is used for the district heat production.

353

3.4 Effect of feedstock moisture content on overall heat utilization efficiency

Overall heat utilization efficiency is defined as

$$\eta_{overall} = \eta_{biocarbon} + \eta_{DH} + \frac{m_{bark} \cdot HHV_{bark} + m_{dust} \cdot HHV_{dust}}{m_{biomass} \cdot HHV_{biomass}} \quad (21)$$

where η – efficiency, m – mass flow rate [kg/h], HHV – higher heating value [MJ/kg dry].

Bark and sawdust (assuming the same composition and heating value as woodchips) are also

1
2
3 359 taken into account when calculating the overall heat utilization efficiency. Note that the
4
5 360 overall efficiency do not include district heat negative efficiency, the meaning with showing
6
7 361 (later) a negative efficiency for district heat is to show that additional external heat is
8
9 362 required to supplement the district heat plant, or alternatively the bark and sawdust could be
10
11 363 burned to maintain the heat production. As shown in Figure 10, the model predicts higher
12
13 364 energy efficiency in the low temperature range (300 – 350 °C), however the quality of the
14
15 365 biocarbon mimics torrefaction quality, which is below 66% fixed carbon content. Overall
16
17 366 heat utilization efficiency decreases almost linearly with increasing pyrolysis temperature.
18
19 367 There is a strong influence of feedstock moisture content on the overall heat utilization
20
21 368 efficiency (Figure 10); increasing moisture content means a higher energy consumption for
22
23 369 drying. Increasing pressure also increases the heat utilization efficiency due to increasing
24
25 370 biocarbon yield.
26
27
28
29
30

31 371

32 372 **4. Techno – economic analysis (TEA)**

33
34 373 The next stage of the model is techno – economic analysis, which allows estimating the
35
36 374 costs associated with production of biocarbon as a function of three parameters: scale of
37
38 375 production and process temperature and pressure. Aspen Plus results developed for the base
39
40 376 case (10 TPD) is based on a fresh logwood moisture content of 40%. TEA analysis is
41
42 377 conducted based on the hierarchical three factors simulation coupled to cost parametric
43
44 378 analysis. Four different scenarios are identified to analyze the biocarbon value chain.
45
46 379 Statistical simulation experiments (Box – Behnken approach) have been used for simulation
47
48 380 of experimental design and the results of mass and energy balances for each scenario are
49
50 381 used as input to the cost modeling. Parametric cost modeling functions are developed using
51
52 382 the cost models based on the three factors Box-Behnken approach. The obtained results
53
54
55
56
57
58
59
60

1
2
3 383 were used to assess economic viability. The TEA modelling method is described in the
4
5 384 flowchart shown in Figure 11.

6
7 385

8 9 10 386 **4.1 Scenario description**

11 387 Four scenarios are identified for the biocarbon value chain studies as shown in

12
13 388

14
15 389

16
17 390

18
19 391

20
21 392 Table 5.

22
23
24 393 Scenario A is based on the transport of logwood from the forest to the plant as shown in

25
26 394 Figure 12. In this scenario, logwood handling is considered similar to the pulp and paper

27
28 395 industries' practices. The feedstock is fresh logwood that is processed in the plant's wood

29
30 396 handling zone involving storage, debarking, chipping and drying, followed by the

31
32 397 carbonization and CHP. Here in this case, pyrolysis vapors, both non-condensable gases and

33
34 398 condensable hydrocarbons are burnt in the CHP plant. The main product of this scenario is

35
36 399 biocarbon. Electricity and district heat are co-products. After internal utilization of steam to

37
38 400 the plant for woodchips drying, the excess heat generated can be sold to nearby industrial

39
40 401 cluster office buildings.

41
42 402 In Scenario B, shown in Figure 13, the woodchips are transported to the plant gate and it is

43
44 403 investigated how far the production cost of biocarbon deviate from scenario A. The wood

45
46 404 handling process steps are woodchips storage and drying (debarking and chipping are

47
48 405 eliminated). All other steps remain the same as in scenario A. The main product is

49
50 406 biocarbon, co-products are electricity and district heat.

51
52 407 In Scenario C the CHP plant is eliminated as shown in Figure 14. Here the pyrolysis vapors

53
54 408 are quenched in the condenser to produce the biooil and this will be sold as a co-product.

55
56
57
58
59
60 17

1
2
3 409 The feedstock is fresh logwood that is processed in the plant pretreatment zone. Pyrolysis
4
5 410 gas is burnt in a gas burner and heat is supplied to the dryer and pyrolysis reactor by indirect
6
7 411 heat exchangers. Excess heat required for the dryer is supplied by the external heat supply
8
9 412 (e.g. burning the bark and sawdust). As well, additional electricity required for the process is
10
11 413 supplied from the grid. This makes sense as rather cheap electricity is available from the
12
13 414 Norwegian hydropower dominated electricity grid. The main products are biocarbon and
14
15 415 biooil. The price for biooil (tar) is set to 500\$/ton according to market price. There is
16
17 416 possibility to cut down Norwegian wood tar import. According to the statistics, the annual
18
19 417 wood tar import is 250 tons³², which is a small amount. However, there are other alternative
20
21 418 markets for tars/biooil, for example extraction of valuable chemicals.
22
23

24
25 419 Scenario D is a copy of scenario A with a change of compression gas. Air is used instead of
26
27 420 nitrogen as it is used in Flash CarbonizationTM by Antal et al.^{29, 30}. This will reduce the costs
28
29 421 associated with the supply of nitrogen. The scenario configuration is shown in Figure 15.
30
31
32 422

33 34 423 **4.2 Purchase equipment and installation costs**

35
36
37
38
39
40
41
42
43
44
45
46
47
48
49
50
51
52
53
54
55
56
57
58
59
60

424 The purchase equipment cost is defined as

$$425 \quad C_{TPEC,i} = C_{S_b,I_b}(S/S_b)^g \quad (22)$$

426 where $C_{TPEC,i}$ is the purchase equipment cost in \$ evaluated for each equipment i , C_{S_b,I_b} is
 427 the base year purchase equipment cost in \$ for base-case equipment size S_b (arbitrary unit),
 428 g is the equipment scale index, S is actual equipment size (in the same arbitrary unit) based
 429 on scale specification.

430 The purchase equipment and installation cost were evaluated based on the function defined
 431 by Kempegowda et al.^{33, 34}, which is a modified version of the Guthrie-Ulrich method³⁵,
 432 and includes pressure, materials and required auxiliary systems, i.e., electric system, piping
 433 and valves, instrumentation and control, through simple multiplication factors.

434 The purchase equipment and installation cost in \$ for each equipment i is defined as:

$$435 \quad C_{S,I,i} = f_{overall}C_{TPEC,i}(I/I_b)k_t^{n-n_b} \quad (23)$$

436 where the cost index I (arbitrary unit) used in this study is based on the Chemical
 437 Engineering Plant Cost Index (CEPCI). It is updated for the year 2015 and I_b is the cost
 438 index (in same arbitrary unit as I) in the base year, $k_t^{n-n_b}$ is the train cost factor since the n^{th}
 439 train is relatively cheaper than the train number n_b of the reference base case because both
 440 can use part of the auxiliary equipment, the parameter k_t is assumed to 0.9³⁶. Overall
 441 installation factor is

$$442 \quad f_{overall} = f_{mat}f_p f_{inst} \quad (24)$$

443 where f_p is the pressure factor, f_{mat} is the material factor and f_{inst} is the installation factor.

444 The installation factor varies based on the type of equipment in the process value chain. This
 445 is evaluated based on equation 25.

$$446 \quad f_{inst} = 1 + f_M[1 + (L/M)k_L] \quad (25)$$

1
2
3 447 with f_M and (L/M) representing installation module factor and labor to module cost ratio
4
5 448 and $k_L = 1.47$ is the labor factor for Norway. Coefficients for each process equipment were
6
7 449 used based on Wood et al.³⁷.
8

9
10 450 Overview of process equipments for the Aspen Plus base scale is shown in
11

12 451

13 452

14 453

15 454

16 455

17 456

18 457

19 458

20 459

21 460

22 461

23 462

24 463

25 464

26 465

27 466

28 467

29 468

30 469

31 470

32 471

33 472

34 473 Table 6.

35

36

37

38

39

1
2
3 474 The cost calculation for the dryer is based on the surface area of each stage in accordance
4
5 475 with equation 26.

6
7 476 $C_{\text{dryer}} = h(15000 + 10500A_d)$ (26)
8

9
10 477 where A_d is the surface area of the dryer in m^2 and h is the number of stages. The cost is
11 478 calculated in \$ in base year 1998. Other factors are presented in

12
13 479

14
15 480

16
17 481

18
19 482

20
21 483

22
23 484

24
25 485

26
27 486

28
29 487

30
31 488

32
33 489

34
35 490

36
37 491

38
39 492

40
41 493

42
43 494

44
45 495

46
47 496

48
49 497

50
51 498

52
53 499

54
55 500

1
2
3
4
5
6
7
8
9
10
11
12
13
14
15
16
17
18
19
20
21
22
23
24
25
26
27
28
29
30
31
32
33
34
35
36
37
38
39
40
41
42
43
44
45
46
47
48
49
50
51
52
53
54
55
56
57
58
59
60

501 Table 6. The cost of the carbonization reactor is calculated based on the weight of vessels,
502 assuming three hot reactors, whereof one heating and one cooling section are used to ensure
503 the continuity of the process. The cost of each reactor is equal

$$504 \quad C_{reactor} = 73f_{cp}W_v^{0.66}\mu \quad (27)$$

505 where f_{cp} is the cost factor, W_v is the weight of one vessel in kg, μ is the total number of
506 vessels. The cost is calculated in \$ in base year 2002. Other factors are presented in

507

508

509

510

511

512

513

514

515

516

517

518

519

520

521

522

523

524

525

526

527

528

1
2
3
4
5
6
7
8
9
10
11
12
13
14
15
16
17
18
19
20
21
22
23
24
25
26
27
28
29
30
31
32
33
34
35
36
37
38
39
40
41
42
43
44
45
46
47
48
49
50
51
52
53
54
55
56
57
58
59
60

529 Table 6. As well,

530

531

532

533

534

535

536

537

538

539

540

541 **Table 7** presents the base scale TPEC costs for the different scenarios based on the cost
542 components involved in the process chains. Purchase equipment cost decreased significantly
543 for scenario C, due to removal of the CHP unit. TPEC for scenario A and D is the same
544 because there is only a change in pressurizing medium.

545

4.3 Total permanent investment

546

1
2
3 547 The total permanent investment [\$] include the cost components outside the battery limit
4
5 548 (OSBL). These are coupled to purchase equipment installation factors through equation 28.
6
7 549 This is based on the work of Kempegowda et al.³³.

$$10 \quad C_{TPI} = (\sum_i C_{S,I,i})[1 + f_{site} + f_{building} + f_{land}][1 + f_{cont} + f_{eng}][1 + f_{dev} + f_{com}] \quad (28)$$

11 where $(\sum_i C_{S,I,i})$ is the total purchase and installation cost in \$, for the overall plant, and f_i
12
13
14 552 represent additional costs factors including civil work associated with site preparation and
15
16
17 553 process-equipment building, offsite accessibility and services, contingency margin,
18
19 554 contractors, land, royalties and patents. Cost factors are shown in

20
21 555

22
23 556

24
25
26 557

27
28 558

29 559

30 560

31 561

32 562

33 563

34 564

35 565

36 566

37 567

38 568

39 569

40 570

41 571

Table 8. Cost associated factors to estimate the Total Permanent Investment (TPI)³³

Factor	Cost associated factors	Typical value	Adopted value
f _{site}	Site preparation	0.05 – 0.2	0.05
f _{building}	Buildings	0.05 – 0.1	0.05
f _{land}	Land	0.05 – 0.1	0.05
f _{cont}	Cost of contingency	0.05 – 0.15	0.05
f _{eng}	Engineering	0.02 – 0.05	0.02
f _{dev}	Project development and	0.02 – 0.03	0.02
f _{com}	Commissioning	0.1	0.1

42
43
44
45
46
47
48
49 572

50
51 573

52
53
54
55
56
57
58
59
60

1
2
3
4
5
6
7
8
9
10
11
12
13
14
15
16
17
18
19
20
21
22
23
24
25
26
27
28
29
30
31
32
33
34
35
36
37
38
39
40
41
42
43
44
45
46
47
48
49
50
51
52
53
54
55
56
57
58
59
60

574 .
575 TPEC is only one part of the total costs associated with plant construction, as shown in
576 Table 7. According to Timmerhaus et al.³⁸ total purchase and installation cost is typically 4
577 – 5 times higher than TPEC for solids processing. In this model the ratio is around 4.5.
578

579 **4.4 Operating expenses**

1
2
3 580 The operating expenses (OPEX) in \$ per annual basis are calculated from

$$4 \quad 581 \quad C_{OPEX} = C_B + C_{op,d} + C_{op,i} + C_{labor} \quad (29)$$

6
7 582 where C_B is cost of biomass supply, $C_{op,d}$ represents the total direct variable, operational
8
9 583 dependent on the annual biomass to biocarbon conversion, $C_{op,i}$ is the fixed indirect
10
11 584 operational costs not directly dependent on the amount of biomass processed but required
12
13 585 for having the plant in activity, and C_{labor} is the labor cost.

14
15
16 586 Labor cost in \$ is calculated based on the exponential function of employed people $E_{ppl,i}$ and
17
18 587 appropriate annual salaries D_i in \$ according to equations 30 and 31.

$$19 \quad 20 \quad 21 \quad 588 \quad C_{labor} = \sum_i E_{ppl,i} D_i \quad (30)$$

$$22 \quad 23 \quad 24 \quad 589 \quad E_{ppl,i} = \left(\frac{P_{act}}{P_{base}} \right)^{b_i} \quad (31)$$

25
26
27 590 where P_{act} is actual biocarbon production in TPD, $P_{base} = 10$ TPD. Base scale labor costs and
28
29 591 their scaling factors are presented in Table 9.

30
31 592 The reference values for the fixed indirect operational costs $C_{op,i}$ are shown in

32
33 593

34
35 594 Table 10. The direct variable operational cost $C_{op,d}$ depends on the used media and the
36
37 595 produced wastes, which are proportional to annual plant operating time. The cost of biomass
38
39 596 supply in \$ can be estimated from

$$40 \quad 41 \quad 42 \quad 597 \quad C_B = (\dot{M}_F t_{prod} / \rho_B) [c_{expl} + c_{chip} + c_{tr,f} + c_{tr,L} L_f] \quad (32)$$

43
44 598 where \dot{M}_F indicates the plant capacity [kg/h] based on the input biomass mass flow rate,
45
46 599 t_{prod} is the annual production time [hours], ρ_B is the input biomass density [kg/m³], c_{expl} is
47
48 600 the forest exploitation cost per unit volume of biomass [\$/m³], c_{chip} is the cost for biomass
49
50 601 chipping and storage per unit volume of biomass [\$/m³], $c_{tr,f}$ is the fixed transport costs per
51
52 602 unit volume of biomass [\$/m³] and $c_{tr,L}$ is the variable (distance-dependent) transport costs
53
54 603 per unit volume and transport distance of biomass [\$/m³/m] and

$$L_f = 2(\dot{M}_F t_{prod}/m_{f,S})^{1/2} \quad (33)$$

is the average biomass transport distance [m], which depends on the annual biomass conversion of the plant, with $m_{f,S}$ as the biomass production per unit area [kg/m^2].

Annual base scale 10 TPD OPEX for the different scenarios is shown in Table 11. Visible differences in the costs arise from the various scenario configurations. In scenario B cost of biomass supply is higher because woodchips used as feedstock is more expensive than logwood. The lowest OPEX is in Scenario D, where air is used instead of expensive nitrogen to pressurize the pyrolysis reactor. Scenario C is characterized by the highest operating expenses due to removal of the CHP unit. The excess heat and electricity must then be purchased externally.

Biomass supply cost comparison: Biomass supply under Norwegian conditions is the largest share of OPEX together with labor cost, as shown in Table 11. Biomass supply variables under Norwegian conditions are shown in Table 12. Two different feedstocks (spruce logwood and spruce woodchips) were compared at different operating conditions (temperature and pressure) and scale of biocarbon production. Replacement of logwood for woodchips resulted in an increased cost in the supply of biomass by 18%, which is independent of the operating conditions. With the increasing of operating pressure from 1 to 10 bar, there is a decrease of biomass supply cost of around 11% in the carbonization temperature range of 450 – 500 °C and at a biocarbon production of 45 – 60 TPD. This attribute is common for all cases, and this is due to the increased yield of biocarbon at elevated pressure in the carbonization temperature range. The details of biomass supply cost in MM\$/year for various carbonization conditions are supplemented as Appendix E.

$$\text{Biomass cost} = x_0 + T x_T + p x_p + W x_W + T^2 x_{TT} + p^2 x_{pp} + W^2 x_{WW} + T p x_{Tp} + T W x_{TW} + p W x_{pW} \quad (34)$$

1
2
3 628 where T is temperature in °C, p is pressure in MPa in this equation, W is scale of biocarbon
4
5 629 production in TPD, and the x coefficients for logwood and woodchips are shown in Table 13.

6
7 630 **Influence on the overall OPEX:** Figure 16(a) and (b) shows the influence of operating
8
9 631 conditions pressure and temperature versus plant scale on the overall operating expenses.
10
11 632 Generally, all cases showed increasing trend for OPEX. Scenario B has higher OPEX, which
12
13 633 is due to higher price of woodchips (284 NOK/m³) supplied to the plant compared to
14
15 634 logwood (236 NOK/m³). It also depends on the biomass share of total operating expenses.
16
17 635 The difference is around 7 – 8.5% (450 – 500 °C, 1 – 10 bar and 60 TPD). In scenario A
18
19 636 increasing pressure from 1 to 10 bar increases OPEX by 6 – 8% (450 – 500 °C and 40 – 60
20
21 637 TPD). Scenario C gives higher OPEX than scenario A, around 50 – 55% increase in the cost
22
23 638 of biocarbon is estimated. This is due to purchase of heat and electricity for the auxiliary
24
25 639 utilities in the plant.
26
27
28
29

30 640

31 32 33 641 **4.5 Economic viability**

34
35 642 Economic viability analysis is carried out for the four scenarios described
36
37 643 in section 4.1. Impact of different process configurations, operating conditions (temperature
38
39 644 in the range 300 – 500 °C and pressure in the range 1 – 10 bar) and scale of biocarbon
40
41 645 production (10 – 60 TPD). The results were compared based on the relative difference
42
43 646 between scenarios B, C, D and reference scenario A according to equation 35.

44
45
46
47 647
$$RD_{\%} = \frac{R_i - R_A}{R_A} \cdot 100 \quad (35)$$

48
49 648 where RD_% is the relative difference in percent, R_i is the result for scenario i (i = B, C, D),
50
51 649 R_A is the result for reference scenario A.

52
53
54 650 Financial parameters are gathered in Table 14. Economic viability is calculated based on 20
55
56 651 years plant lifetime with plant operating factor 85% (7446 hours/year). The equipment is

1
2
3 652 depreciated according to a straight line depreciation model during a 20 years period. The
4
5 653 investment is financed 30% by equity and 70% by loan. Loan repayment period is set to 10
6
7 654 years with 7% interest rate. The total permanent investment cost (TPI) is updated to US\$
8
9 655 (2015) based on Chemical Engineering Plant Cost Index (CEPCI 2015). According to
10
11 656 Norwegian condition income tax rate is 28%.

12
13
14 657 **Specific plant cost comparison:** Specific plant cost TPEC/kW biocarbon output is the cost
15
16 658 associated with the purchased equipments expressed as the cost per unit of product output.
17
18 659 Influence of carbonization process conditions (pressure and temperature) on the TPEC
19
20 660 versus various plant capacities are shown in Figure 17(a), (b) and (c). TPEC follows the
21
22 661 scale of economics rules and shows decreasing trend with increasing plant capacity ³³.
23
24 662 Scenario B is around 1 – 8% cheaper compared to scenario A, this is due to scenario A
25
26 663 having more functional units for handling the logwood (debarker and chipper).

27
28
29 664 **Influence of pressure:** Elevated pressure in the reactor decreased TPEC, increasing pressure
30
31 665 from 1 to 10 bar (Figure 17(a)) decreases the TPEC around 10% in the temperature range of
32
33 666 450 – 500 °C and for 60 TPD. This attribute is due to the increased biocarbon yield at
34
35 667 elevated pressures. TPEC for scenario C is decreasing relatively to scenario A, the cost
36
37 668 reduction is around 5 – 6% for 10 bar, 450 – 500 °C and 60 TPD and 12% for 1 bar, 450 –
38
39 669 500 °C and 60 TPD. The reason for such decrease is elimination of the CHP unit in scenario
40
41 670 C and production of biooil as a co-product. Pyrolysis gases are burnt in the gas burner and
42
43 671 produced heat is utilized for the drying and pyrolysis reactor. The associated cost is based on
44
45 672 the burner configuration rather on the complete CHP unit. Scenario D is not shown because
46
47 673 it has the same cost as Scenario A, the difference is only in OPEX (air instead of nitrogen).

48
49
50 674 **Influence of temperature:** Similarly, influence of carbonization temperature (300 °C to 500
51
52 675 °C) on TPEC are shown in Figure 17(b) and (c). Increasing temperature increases the plant
53
54 676 specific TPEC, which is due to a decreasing biocarbon yield at the same pressure, shown for
55
56
57
58
59
60

1
2
3 677 1 bar in Figure 17(b) and 10 bar in Figure 17(c). TPEC almost doubles at high temperature,
4
5 678 however, the quality of biocarbon produced at low temperature carbonization may not be
6
7 679 suitable to replace coke as a reductant, which is due to the high volatiles content and the low
8
9 680 fixed carbon content.

11 681 **Cost of biocarbon:** Cost of biocarbon [\$/GJ] is evaluated over the entire lifetime of the
12
13 682 plant, assuming that the project is financed 100% from loan, and is calculated from equation
14
15 683 36.

$$16 \quad C_{\text{biocarbon}} = \frac{\sum_{u=1}^U [\beta^u (C_{TPI,u} + C_{OPEX,u} - C_{IN,u})]}{\sum_{u=1}^U HHV_{\text{biocarbon}} \cdot p_{bc,u}} \quad (36)$$

18
19 684 where u is the year starting from the plant construction, U is the plant lifetime in years,
20
21 685 $\beta = 1/(1 + r)$ is the discount factor which represents time value of money, r is the interest
22
23 686 rate. $C_{TPI,u}$ is the annual permanent investment cost in \$, $C_{OPEX,u}$ is the annual operating
24
25 687 expenses in \$, $C_{IN,u}$ is the annual income in \$ from selling co-products (electricity, heat,
26
27 688 bark, sawdust and CO₂ replacement), however, in our TEA analysis, the bark and sawdust
28
29 689 are not included in the evaluation. $HHV_{\text{biocarbon}}$ is the HHV of produced biocarbon [MJ/kg
30
31 690 dry biocarbon], $p_{bc,u}$ is the annual biocarbon production [ton]. The annual operational
32
33 691 income in \$ is calculated from equation 37.

$$34 \quad C_{IN,u} = C_{el,u} + C_{heat,u} + C_{CO_2,u} \quad (37)$$

35
36 692 where $C_{el,u}$ is annual income in \$ from selling electricity, $C_{heat,u}$ is annual income in \$ from
37
38 693 selling heat, $C_{CO_2,u}$ is annual income in \$ from replacement of fossil fuel to renewable based
39
40 694 on avoided CO₂ emission. Reference values are shown in Table 15.

41
42 695 Influence of operating conditions on the cost of biocarbon: The cost of biocarbon is the
43
44 696 decision parameter for evaluating the economic viability of the biocarbon production
45
46 697 scenarios based on the current market conditions. The economic viability is estimated for
47
48 698 the scenarios A, B, C and D at operating temperatures 300 – 500°C and pressures 1 – 10 bar
49
50 699

1
2
3 701 and for scale of biocarbon production of 10 to 60 TPD. The results are shown in Figure 18,
4
5 702 Figure 19 and Figure 20.

6
7 703 Increasing pressure from 1 bar to 10 bar in Scenario A results in increased biocarbon cost
8
9 704 (Figure 18). The increase is ~10% in the lower temperature range (300 °C) where the price
10
11 705 increased from ~10.5 \$/GJ to ~11.5 \$/GJ and ~1.5% at a temperature of 500 °C where the
12
13 706 price increased from ~14 \$/GJ to ~14.3 \$/GJ, which is at the production scale of 50 – 60
14
15 707 TPD (Figure 18). Similar costs were estimated for Finnish conditions for torrefaction and
16
17 708 for charcoal production³⁹. Increasing pressure in the carbonization reactor at high
18
19 709 temperature carbonization does not increase the cost significantly (Figure 18), this is due to
20
21 710 the higher yield of biocarbon with increasing pressure.

22
23
24
25 711 Scenario C shows a large decrease in the production cost of biocarbon compared to scenario
26
27 712 A (Figure 18), around 40 – 44% (**1 bar**, 450 – 500 °C and 40 – 60 TPD) the estimated price
28
29 713 is ~8 \$/GJ and around 30 – 36% (**10 bar**, 450 – 500 °C and 40 – 60 TPD) the estimated
30
31 714 price is ~9.3 \$/GJ. This is due to the advantage of co-production of biooil at the market price
32
33 715 500 \$/ton. Increasing pressure in this case results in decrease of biooil yield, according to
34
35 716 secondary pyrolysis reactions, which results in higher biocarbon and gas yields.

36
37
38 717 Supply of woodchips to the plant is increasing the cost of biocarbon for scenario B as shown
39
40 718 in Figure 19. In comparison to the logwood purchasing scenario, there is direct purchase of
41
42 719 woodchips to the plant at higher cost, the relative difference of production cost is around 5%
43
44 720 compared to scenario A (**1 bar**, 450 – 500 °C and 55 – 60 TPD) with biocarbon price ~14.5
45
46 721 \$/GJ and around 4% higher compared to scenario A (**10 bar**, 450 – 500 °C, 55 – 60 TPD)
47
48 722 with biocarbon price 14.7 \$/GJ. An interesting observation is that for the base scale, where
49
50 723 the production is 10 TPD and the temperature range below 400 °C, there is an advantage of
51
52 724 woodchips purchase to the plant by ~1% decrease in production cost (Figure 19), the
53
54 725 biocarbon price is ~18 \$/GJ. However, the grade of biocarbon produced at these conditions
55
56
57
58
59
60

1
2
3 726 is not suitable for metallurgical industries, this is because of the low fixed carbon content in
4
5 727 the product.

6
7 728 When air is used to pressurize the reactor (scenario D), there is a decrease in biocarbon
8
9 729 production cost of around 8% (Figure 20) compared to scenario A at 1 bar and scenario D at
10
11 730 10 bar at 500 °C and production scale 60 TPD, where the price is reduced from ~14 \$/GJ to
12
13 731 ~13\$/GJ, Figure 20. This attribute is due to the compression energy consumption
14
15 732 differences.

16
17
18 733 Influence of biomass transportation distance: Scenario A and D are considered for studying
19
20 734 the influence of transport distance. Modelling results suggests that a carbonization
21
22 735 temperature of 500 °C is suitable to achieve highest fixed carbon content (81%)²⁶. Thus, the
23
24 736 obtained biocarbon can be widely used in metallurgical industry as a reductant. In order to
25
26 737 minimize the cost of production, a scale of production of 60 TPD is chosen for transportation
27
28 738 cost analysis. The influence of biomass transportation distance on biocarbon production cost
29
30 739 is shown in Figure 21Figure 21.

31
32
33
34 740 The cost of logwood is increasing with transportation distance according to a linear
35
36 741 correlation. Under Norwegian conditions fresh woody biomass costs 4.75 \$/GJ for a 20 km
37
38 742 transportation distance and it is increasing up to 7.15 \$/GJ when the transportation distance
39
40 743 is 220 km, Figure 21(a). Therefore, it is reasonable to transport biomass up to several tens of
41
42 744 kilometers. The plant location should be properly selected to avoid additional cost and
43
44 745 emissions related with biomass transportation. Figure 21(b) shows the influence of biomass
45
46 746 transport on biocarbon production cost for scenario A and Figure 21(c) for scenario D.
47
48 747 Increasing pressure additionally increases the cost of biocarbon production.

49
50
51 748 Economic viability on selling price of biocarbon product: Internal rate of return (IRR) is
52
53 749 used as a financial viability indicator to analyze the project viability. It is defined as the
54
55 750 discount rate that would make the net present value (NPV) of the investment equal to zero.

1
2
3 751 Project IRR for scenario A, B and C is selected for analyzing the (500 °C, 60 TPD biocarbon
4
5 752 production) economics at 70% debt as shown in Figure 21(d). The highest IRR achieves
6
7 753 scenario C, where biooil is a co-product, it is due to high market price of woody tar at
8
9 754 500\$/ton. The IRR decrease at elevated pressure according to lower biooil yield. The
10
11 755 difference between scenario A and D is related to the difference in pressurizing agent
12
13 756 (nitrogen and air).
14
15
16
17

18 758 **5. Conclusions**

19
20
21 759 Detailed simulation of the biocarbon production value chain consisting of logwood handling,
22
23 760 debarking, chipping, drying, carbonization, and combined heat and power production plant
24
25 761 was developed using Aspen Plus. Carbonization process yields (product yields) are predicted
26
27 762 with a multifunctional model considering pressure, temperature and particle size effects. The
28
29 763 empirical correlation indicates a strong influence of temperature as well as a significant
30
31 764 influence of pressure and particle size on the biocarbon yield. As well, biocarbon energy
32
33 765 efficiency is higher in the low temperature carbonization regime, however, the biocarbon
34
35 766 quality with respect to fixed carbon content is lower in the low temperature carbonization
36
37 767 regime. For high temperature carbonization, above 400°C, increasing pressure in the
38
39 768 carbonization reactor increases the fixed carbon yield.
40
41
42

43 769 Feedstock moisture content has strong influence on district heat efficiency. For the fresh
44
45 770 wood having 60% moisture, both district heat efficiency and steam export is negative, since
46
47 771 all the low-pressure steam is consumed for thermal drying of the feedstock, which has a
48
49 772 penalty of 5-10% of the HHV of input feedstock. A parametric function for district heat
50
51 773 production is developed for the carbonization process parameters (temperature, pressure) and
52
53 774 production scale. Techno-economic analysis was conducted for the four case scenarios,
54
55
56 775 Scenario A is based on logwood transport from the forest to the plant gate with biocarbon as
57
58
59
60

1
2
3 776 the main product and district heat and electricity as the co-products. Scenario B is based on
4
5 777 the supply of woodchips to the plant with biocarbon as the main product and district heat and
6
7 778 electricity as the co-products. Scenario C is based on the biocarbon as a main product and
8
9
10 779 biooil as co-product. In Scenario D nitrogen is replaced with air as inert agent air in the
11
12 780 carbonization reactor.

13
14 781 A novel approach for a parametric cost modelling function for the overall plant design is
15
16 782 developed based on a statistical approach using the Box and Behnken technique to the study
17
18 783 the influence of scale and operating variables (temperature and pressure). TEA reveals that
19
20 784 specific plant cost (TPEC) can be reduced by reducing wood handling (scenario B) by
21
22 785 supplying woodchips in the range of 1-8% in comparison to scenario A. Also, there is a
23
24 786 decrease in total purchase equipment cost (TPEC) with increasing pressure by (Scenario A)
25
26 787 ~10% (from 1 to 10 bar, 450-500, 60 TPD), because of the higher pressure effect on the
27
28 788 biocarbon yield. Moreover, increasing scale of production results in decreasing specific
29
30 789 TPEC, which follows the scale of economics rule. Specific TPEC cost in Scenario C is
31
32 790 decreased by 5-6% (for 10 bar, 450-500°C, 60 TPD) and 12% (1 bar, 450-500°C, 60 TPD) as
33
34 791 compared to scenario A. The major share of OPEX is the biomass feedstock price. Overall
35
36 792 OPEX cost is higher in scenario B where woodchips are purchased at market rate. The
37
38 793 difference is around 7-8.5% (450-500°C, 1-10 bar, 50-60 TPD). In Scenario A, increasing
39
40 794 pressure from 1 bar to 10 bar increased OPEX ~6-8% (450-500°C, 40-60 TPD). Scenario C
41
42 795 gives higher OPEX than scenario B, around 50-55% due to purchase of heat and electricity.
43
44 796 Cost of biocarbon production (\$/GJ) is higher in Scenario B than Scenario A by ~5% (1 bar,
45
46 797 450 -500°C, 55-60 TPD) and ~4% (10 bar, 450-500°C, 55-60 TPD). There is an advantage
47
48 798 of woodchips purchase by ~1% regarding production cost at lower scale for the base scale of
49
50 799 10 TPD and carbonization temperature below 400°C. In Scenario A increasing pressure
51
52 800 from 1 bar to 10 bar increased production cost of biocarbon (\$/GJ), with ~9.7% at a
53
54
55
56
57
58
59
60

1
2
3 801 temperature of 300°C and 1.3% at 500°C, both in the production range of 50-60 TPD, which
4
5 802 can be regarded as insignificant.

6
7 803 Scenario C, with biooil as co-product, exhibits a large decrease in the production cost of
8
9 804 biocarbon (\$/GJ) of 40-44% (1 bar, 450-500°C, 40-60 TPD) and 30-36% (10 bar, 450-
10
11 805 500°C, 40-60 TPD).

12
13
14 806 However, increasing the pressure from 1 bar to 10 bar decreased the yield of biooil due to
15
16 807 increased biocarbon yields at elevated pressure. Under Norwegian conditions, supply of
17
18 808 woodchips instead of logwood to the plant gate increases the supply cost of biomass by 18%
19
20 809 (independent of the operating conditions).

21
22
23 810 Cost of biomass supply increased from 4.75 \$/GJ to 7.15 \$/GJ by increasing the
24
25 811 transportation distance of logwood supply from forest to the plant gate from 20 to 220 km.

26
27 812 This also suggest that cost of biocarbon production increase linearly at a rate of 0.5 \$/GJ for
28
29 813 every 40 km transport distance for the best selected case for metallurgical industry (60 TPD
30
31 814 at 500°C). Case D with pressurization of the carbonization reactor with air decreased the
32
33 815 cost of biocarbon by ~1 \$/GJ in comparison with nitrogen at the same operating conditions.

34
35
36 816 Pressurization by air reduced the cost of biocarbon by 0.5 \$/GJ at 5 bar and 1 \$/GJ at 10 bar
37
38 817 for the same transport distance of forest logwood. Finally, the economic return based on
39
40 818 IRR suggests that highest IRR achieved for scenario C, where biooil is a co-product, which
41
42 819 is due to high market price of woody tar at 500 \$/ton. Finally, the TEA reveals the influence
43
44 820 of different grades of biocarbon, i.e. different fixed carbon contents, for metallurgical and
45
46 821 cofiring applications. Higher grades of biocarbon increases the cost of production of
47
48 822 biocarbon, however, for metallurgical industries a relatively high grade is needed.

49
50
51
52 823

53
54 824 **Acknowledgements**

1
2
3 825 The authors acknowledge the financial support from the Research Council of Norway, and
4
5 826 the industrial partners (Elkem AS, Department Elkem Technology; Norsk Biobrensel AS;
6
7 827 AT Skog SA; Eyde-nettverket; Saint Gobain Ceramic Materials AS; Eramet Norway AS;
8
9 828 Alcoa Norway ANS) in the BioCarb+ project.
10
11
12 829
13
14 830
15
16 831
17
18 832
19
20 833
21
22 834

References

- 23
24
25 835 1. SSB Energy use in the manufacturing sector, Statistics Norway [https://www.ssb.no/en/energi-og-](https://www.ssb.no/en/energi-og-industri/statistikker/indenergi/aar/2016-06-17)
26 836 [industri/statistikker/indenergi/aar/2016-06-17](https://www.ssb.no/en/energi-og-industri/statistikker/indenergi/aar/2016-06-17)
27 837 2. Scarlet, N.; Dallemand, J.-F.; Skjelhaugen, O. J.; Asplund, D.; Nesheim, L., An overview of the biomass
28 838 resource potential of Norway for bioenergy use. *Renewable and Sustainable Energy Reviews* **2011**, *15*, (7),
29 839 3388-3398.
30 840 3. Belbo, H.; Talbot, B., Systems Analysis of Ten Supply Chains for Whole Tree Chips. *Forests* **2014**, *5*,
31 841 (9), 2084-2105.
32 842 4. Lucas, L. H. M. Effect of pressure on the characteristics of biomass pyrolysis. Ph.D thesis., University
33 843 of Newcastle. Faculty of Engineering and Built Environment, School of Engineering, 2012.
34 844 5. Mohan, D.; Pittman, C. U.; Steele, P. H., Pyrolysis of Wood/Biomass for Bio-oil: A Critical Review.
35 845 *Energy & Fuels* **2006**, *20*, (3), 848-889.
36 846 6. de Oliveira Vilela, A.; Lora, E. S.; Quintero, Q. R.; Vicintin, R. A.; Pacceli da Silva e Souza, T., A new
37 847 technology for the combined production of charcoal and electricity through cogeneration. *Biomass and*
38 848 *Bioenergy* **2014**, *69*, 222-240.
39 849 7. Antal, M. J.; Mok, W. S. L.; Varhegyi, G.; Szekely, T., Review of methods for improving the yield of
40 850 charcoal from biomass. *Energy & Fuels* **1990**, *4*, (3), 221-225.
41 851 8. FAOSTAT Forestry Production and Trade. <http://faostat3.fao.org/download/F/FO/E> (25th August),
42 852 9. Antal, M. J.; Grønli, M., The art, science, and technology of charcoal production. *Industrial &*
43 853 *Engineering Chemistry Research* **2003**, *42*, (8), 1619-1640.
44 854 10. Demirbas, A., Carbonization ranking of selected biomass for charcoal, liquid and gaseous products.
45 855 *Energy Conversion and Management* **2001**, *42*, (10), 1229-1238.
46 856 11. Violette, M., Memoire sur les Charbons de Bois. *Ann. Chim. Phys* **1853**, *32*, 304.
47 857 12. Antal, M. J.; Croiset, E.; Dai, X.; DeAlmeida, C.; Mok, W. S.-L.; Norberg, N.; Richard, J.-R.; Al Majthoub,
48 858 M., High-yield biomass charcoal. *Energy & Fuels* **1996**, *10*, (3), 652-658.
49 859 13. Wang, L.; Skreiberg, Ø.; Gronli, M.; Specht, G. P.; Antal, M. J., Is Elevated Pressure Required to
50 860 Achieve a High Fixed-Carbon Yield of Charcoal from Biomass? Part 2: The Importance of Particle Size. *Energy &*
51 861 *Fuels* **2013**, *27*, (4), 2146-2156.
52 862 14. Van Wesenbeeck, S.; Wang, L.; Ronsse, F.; Prins, W.; Skreiberg, Ø.; Antal, M. J., Charcoal "Mines" in
53 863 the Norwegian Woods. *Energy & Fuels* **2016**.
54 864 15. Deev, A.; Jahanshahi, S. In *Development of a pyrolysis technology to produce large quantities of*
55 865 *charcoal for the iron and steel industry*, 6th International Congress on the Science and Technology of
56 866 Ironmaking, 2012; 2012; pp 1132-1142.

- 1
2
3 867 16. Jahanshahi, S.; Mathieson, J. G.; Somerville, M. A.; Haque, N.; Norgate, T. E.; Deev, A.; Pan, Y.; Xie, D.;
4 868 Ridgeway, P.; Zulli, P., Development of Low-Emission Integrated Steelmaking Process. *Journal of Sustainable*
5 869 *Metallurgy* **2015**, 1, (1), 94-114.
6 870 17. Brown, N. J.; Bastien, L. A. J.; Price, P. N., Transport properties for combustion modeling. *Progress in*
7 871 *Energy and Combustion Science* **2011**, 37, (5), 565-582.
8 872 18. Peng, D.-Y.; Robinson, D. B., A New Two-Constant Equation of State. *Industrial & Engineering*
9 873 *Chemistry Fundamentals* **1976**, 15, (1), 59-64.
10 874 19. Michael Suhr, e. a., Best Available Techniques (BAT) Reference Document for the Production of Pulp,
11 875 Paper and Board. In Studies, I. f. P. T., Ed. European Commission: 2015.
12 876 20. Kollmann, F. F. P.; Kuenzi, E. W.; Stamm, A. J., Principles of Wood Science and Technology - II Wood
13 877 Based Materials. **1975**.
14 878 21. Monsen, B.; Gronli, M.; Nygaard, L.; Tveit, H., The use of biocarbon in Norwegian ferroalloy
15 879 production. **2001**
- 16 880
17 881 22. Laitila, J.; Asikainen, A.; Ranta, T., Cost analysis of transporting forest chips and forest industry by-
18 882 products with large truck-trailers in Finland. *Biomass and Bioenergy* **2016**, 90, 252-261.
19 883 23. Johansson, A.; Fyhr, C.; Rasmuson, A., High temperature convective drying of wood chips with air and
20 884 superheated steam. *International Journal of Heat and Mass Transfer* **1997**, 40, (12), 2843-2858.
21 885 24. Scheepers, G.; Wiberg, P.; Johansson, J., A method to estimate wood surface moisture content during
22 886 drying. *Maderas. Ciencia y tecnología* **2017**, (AHEAD), 0-0.
23 887 25. Somerville, M.; Jahanshahi, S., The effect of temperature and compression during pyrolysis on the
24 888 density of charcoal made from Australian eucalypt wood. *Renewable Energy* **2015**, 80, 471-478.
25 889 26. Neves, D.; Thunman, H.; Matos, A.; Tarelho, L.; Gómez-Barea, A., Characterization and prediction of
26 890 biomass pyrolysis products. *Progress in Energy and Combustion Science* **2011**, 37, (5), 611-630.
27 891 27. Aslan, N.; Cebeci, Y., Application of Box-Behnken design and response surface methodology for
28 892 modeling of some Turkish coals. *Fuel* **2007**, 86, (1), 90-97.
29 893 28. Noumi, E. S.; Blin, J.; Valette, J.; Rousset, P., Combined effect of pyrolysis pressure and temperature
30 894 on the yield and CO₂ gasification reactivity of acacia wood in macro-TG. *Energy & Fuels* **2015**, 29, (11), 7301-
31 895 7308.
32 896 29. Antal, M. J.; Mochidzuki, K.; Paredes, L. S., Flash Carbonization of Biomass. *Industrial & Engineering*
33 897 *Chemistry Research* **2003**, 42, (16), 3690-3699.
34 898 30. Antal, M. J. Flash Carbonization™ Process. <http://www.hnei.hawaii.edu/node/219> (25th August),
35 899 31. Turnell, J. R.; Faulkner, R. D.; Hinch, G. N., Recent advances in Australian broiler litter utilisation.
36 900 *World's Poultry Science Journal* **2007**, 63, (2), 223-231.
37 901 32. Bridgwater, A. V., *Advances in thermochemical biomass conversion*. 1994; Vol. 1.
38 902 33. Kempegowda, R. S.; del Alamo, G.; Berstad, D.; Bugge, M.; Matas Güell, B.; Tran, K.-Q., CHP-
39 903 Integrated Fischer-Tropsch Biocrude Production under Norwegian Conditions: Techno-Economic Analysis.
40 904 *Energy & Fuels* **2015**, 29, (2), 808-822.
41 905 34. Kempegowda, R. S.; Pannir Selvam, P.; Skreiberg, Ø.; Tran, K. Q., Process synthesis and economics of
42 906 combined biomethanol and CHP energy production derived from biomass wastes. *Journal of Chemical*
43 907 *Technology and Biotechnology* **2012**, 87, (7), 897-902.
44 908 35. Uhl, V. W., A guide to chemical engineering process design and economics, by Gail D. Ulrich, John
45 909 Wiley & Sons, New York, Chichester, Brisbane, Toronto, Singapore "1984" 472 pages. \$35.95. *AIChE Journal*
46 910 **1984**, 30, (6), 1036-1036.
47 911 36. Larson, E. D.; Jin, H.; Celik, F. E., Large-scale gasification-based coproduction of fuels and electricity
48 912 from switchgrass. *Biofuels, Bioproducts and Biorefining* **2009**, 3, (2), 174-194.
49 913 37. Woods, D. R., *Rules of Thumb*. 2007; p 478.
50 914 38. Peters, M. S.; Timmerhaus, K. D.; West, R. E.; Timmerhaus, K.; West, R., *Plant design and economics*
51 915 *for chemical engineers*. 5th ed.; McGraw-Hill New York: 2003
- 52 916
53 917
54 918 Vol. 4.
55 919 39. Suopajarvi, H.; Pongrácz, E.; Fabritius, T., Bioreducer use in Finnish blast furnace ironmaking –
56 919 Analysis of CO₂ emission reduction potential and mitigation cost. *Applied Energy* **2014**, 124, 82-93.

- 1
2
3 920 40. Hamelinck, C. N.; Faaij, A. P. C., Future prospects for production of methanol and hydrogen from
4 921 biomass. *Journal of Power Sources* **2002**, 111, (1), 1-22.
5 922 41. Towler, G. P.; Sinnott, R. K., *Chemical engineering design: principles, practice, and economics of plant*
6 923 *and process design*. Elsevier: 2013.
7
8 924
9
10 925
11
12 926
13
14 927
15
16 928
17
18 929
19
20 930
21
22 931
23
24 932
25
26 933
27
28 934
29
30
31

 Nomenclature

\dot{M}_F	Plant capacity based on the input biomass mass flow rate (kg/h)
A_d	Dryer surface area (m ²)
b_i	Scaling factor (-)
C_{S_b, I_b}	Purchase cost of base scale equipment (\$)
C_B	Cost of biomass supply (\$)
$C_B, C_{Op,d}, C_{Op,i}, C_{labor}, C_{OPEX}$	Cost biomass, direct operating expenses, indirect expenses, cost of labor, annual operating expenses (\$)
$C_{biocarbon}$	Cost of biocarbon (\$/GJ)
c_{chip}	Biomass chipping and storage cost (\$/m ³)
$C_{CO_2,u}$	Annual income from replacement of fossil fuel to renewable based on avoided CO ₂ emission (\$)
C_{dryer}	Cost of dryer (\$)
$C_{el,u}$	Annual income from selling electricity (\$)
c_{expl}	Forest exploitation cost (\$/m ³)
$C_{heat,u}$	Annual income from selling heat (\$)
$C_{IN,u}$	Annual income from selling co-products (\$)
$C_{OPEX,u}$	Annual operating expenses (\$)
$C_{reactor}$	Cost of carbonization reactor (\$)
$C_{S,i}$	Purchase cost of actual equipment (\$)
$C_{TPEC,i}$	Total purchase cost of equipment (\$)
$C_{TPI,u}$	Annual permanent investment cost (\$)
C_{TPI}	Total permanent investment (\$)
$c_{tr,f}$	Fixed transport cost (\$/m ³)
$c_{tr,L}$	Variable transport cost (\$/m ³ /m)
D_i	Annual salaries (\$)
$E_{ppl,i}$	Number of employed people
f_{cp}	Cost factor (-)

1		
2		
3	f_M	Installation module factor (-)
4	f_{mat}, f_p, f_{inst}	Material factor, pressure factor, installation factor (-)
5	$f_{overall}$	Overall installation factor (-)
6	$f_{site}, f_{building}, f_{land}, f_{cont}, f_{eng}, f_{dev}, f_{com}$	Site factor, building construction factor, land factor, contingency factor, engineering factor, development fee, commissioning factor (-)
7	HHV_{bark}	Higher heating value of bark (MJ/kg dry)
8	$HHV_{biocarbon}$	Higher heating value of biocarbon (MJ/kg dry)
9	$HHV_{biomass}$	Higher heating value of biomass (MJ/kg dry)
10	HHV_{dust}	Higher heating value of dust (MJ/kg dry)
11	I_b	Base year cost index (same arbitrary unit as I)
12	k_L	Labor factor (-)
13	k_t^{n-nb}	Equipment train factor (-)
14	L_f	Average biomass transport distance (m)
15	LHV_{Gas}	Gas lower heating value (MJ/kg)
16	m_{bark}	Mass flow rate of dry bark (kg/h)
17	$m_{biocarbon}$	Mass flow rate of dry biocarbon (kg/h)
18	$m_{biomass}$	Mass flow rate of dry biomass (kg/h)
19	m_{dust}	Mass flow rate of dry sawdust (kg/h)
20	m_{FS}	Biomass production per unit area (kg/m ²)
21	$M_{IN-CHIP}$	Mass flow rate into the chipper (kg/h)
22	M_{LOG}	Logwood mass flow rate (kg/h)
23	n_b	Base case train cost factor (-)
24	P_{act}	Actual production (arbitrary unit)
25	P_{base}	Base scale production (same arbitrary unit as P_{act})
26	$P_{bc,u}$	Annual biocarbon production (ton)
27	P_{CH}	Power consumption chipper (kW)
28	P_{DE}	Power consumption for debarker (kW)
29	P_{el}	Electricity output from CHP (kW)
30	Q_{DH}	District heat thermal power (MJ/h)
31	$RD_{\%}$	Relative difference in percent
32	R_i	Result for scenario i (arbitrary unit)
33	R_A	Result for scenario A (same arbitrary unit as R_i)
34	S_b	Base equipment scale (same arbitrary unit as S)
35	S_{CH}	Static load Chipper (kg/h)
36	S_{DE}	Static load Debarker (kg/h)
37	t_{prod}	Annual production time (hours)
38	W_v	Weight of one vessel (kg)
39	X_{CH}	Chipper electricity consumption for static load (kW)
40	X_{DE}	Debarker electricity consumption for static load (kW)
41	$Y_{biocarbon}$	Biocarbon yield (kg/kg dry biomass)
42	$Y_{C,biomass}$	Carbon content in biomass (kg/kg dry ash free biomass)
43	$Y_{C,tar}$	Carbon content in tar (kg/kg dry tar)
44	$Y_{C,BC}$	Weight fraction of carbon in produced biocarbon, dry ash free basis (-)
45	Y_{CH4}	Gas yield of CH ₄ (kg/kg dry ash free biomass)
46	Y_{CO}	Gas yield of CO (kg/kg dry ash free biomass)
47	y_{fc}	Fixed carbon yield (kg/kg dry ash free biomass)
48	$Y_{H,BC}$	Weight fraction of hydrogen in produced biocarbon, dry ash free basis (-)
49	$Y_{H,biomass}$	Hydrogen content in biomass (kg/kg dry ash free biomass)
50	$Y_{H,tar}$	Hydrogen content in biomass (kg/kg dry tar)
51	Y_{H2}	Gas yield of H ₂ (kg/kg dry ash free biomass)
52	$Y_{O,BC}$	Weight fraction of oxygen in produced biocarbon, dry ash free basis (-)
53	$Y_{O,biomass}$	Oxygen content in biomass (kg/kg dry ash free biomass)
54	$Y_{O,tar}$	Oxygen content in biomass (kg/kg dry tar)
55	$Y_{overall}$	Overall heat utilization efficiency
56	Z_{cr}	Critical moisture content on dry basis (kg/kg)
57	Z_{eq}	Equilibrium moisture content on dry basis (kg/kg)
58	$\eta_{biocarbon}$	Biocarbon energy efficiency (MW biocarbon/MW biomass)
59	η_{DH}	District heat efficiency (MW district heat/MW biomass)
60	η_{el}	Electricity generation efficiency (MW electricity/MW biomass)
	ρ_B	Input biomass density (kg/m ³)
	μ	Number of vessels

1
2
3
4
5
6
7
8
9
10
11
12
13
14
15
16
17
18
19
20
21
22
23
24
25
26
27
28
29
30
31
32
33
34
35
36
37
38
39
40
41
42
43
44
45
46
47
48
49
50
51
52
53
54
55
56
57
58
59
60

A	Ash content in biomass (kg/kg dry biomass)
d	Particle diameter (mm)
FC	Fixed carbon content in biocarbon (kg/kg dry biocarbon)
g	Equipment scale index (-)
h	Number of dryer stages
I	Cost index (arbitrary unit)
L/M	Labor to module cost ratio (-)
n	Train cost factor (-)
p	Pressure (bar)
r	Interest rate
S	Actual equipment size (arbitrary unit)
T	Temperature (°C)
U	Plant lifetime in years
$v(\alpha)$	Normalized drying curve (-)
Z	Current moisture content on dry basis (kg/kg)
α	Normalized moisture content (-)
β	Discount factor
Subscripts	
i	Equipment index

935

936

937

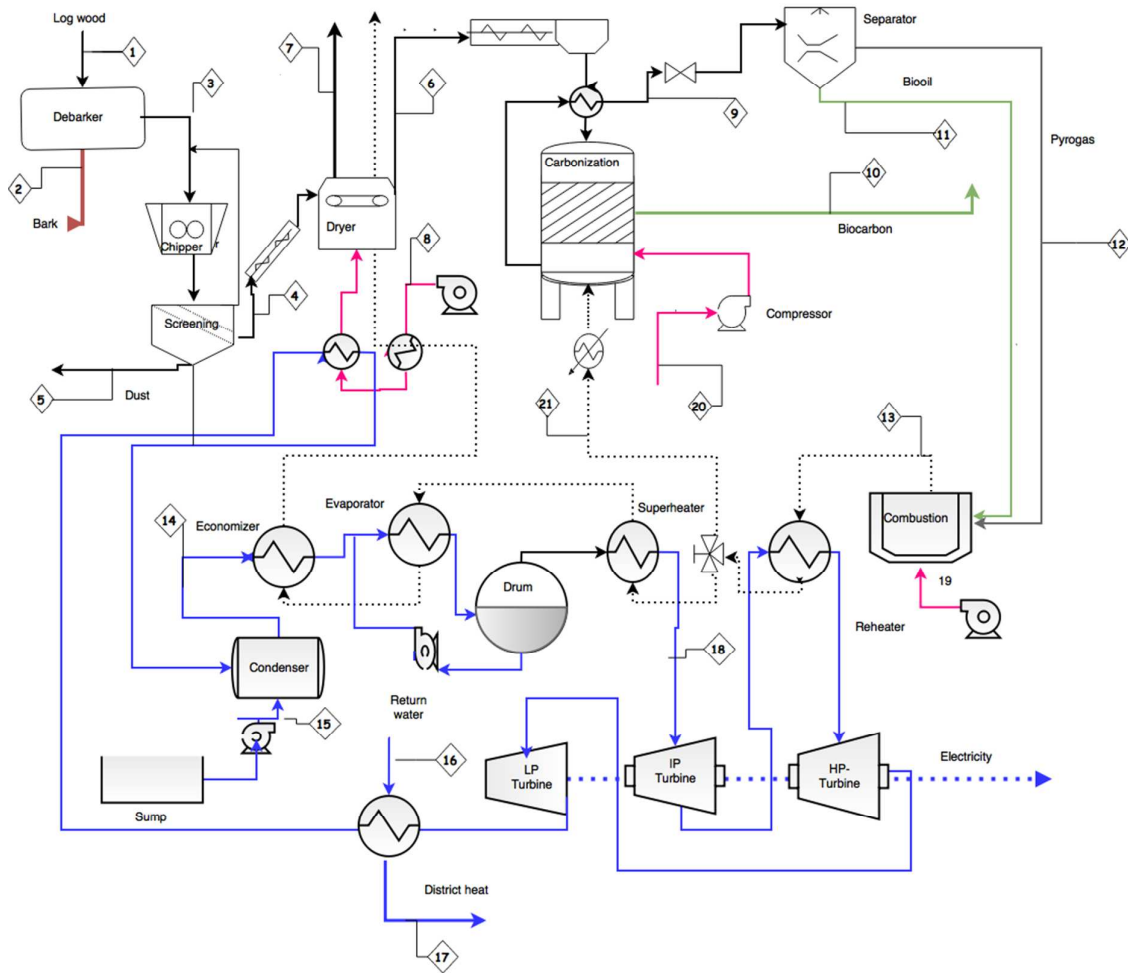
938

939

940

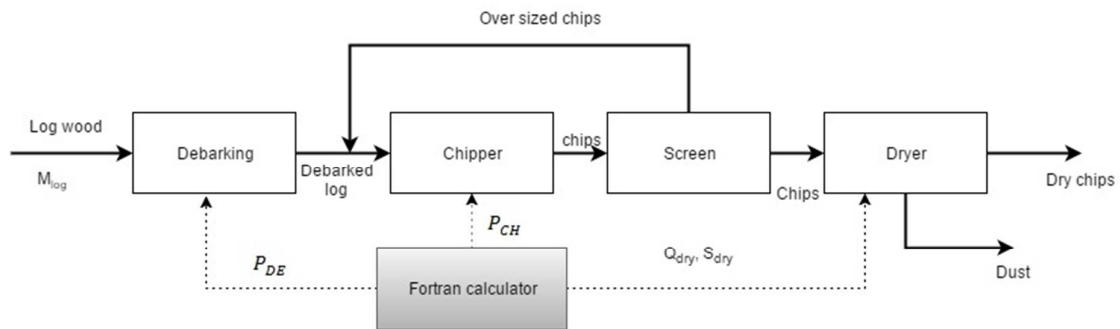
941 **List of Figures**

942



943

944 **Figure 1.** Biocarbon production process flow diagram



945

946 **Figure 2.** Aspen Plus model for logwood handling and thermal drying

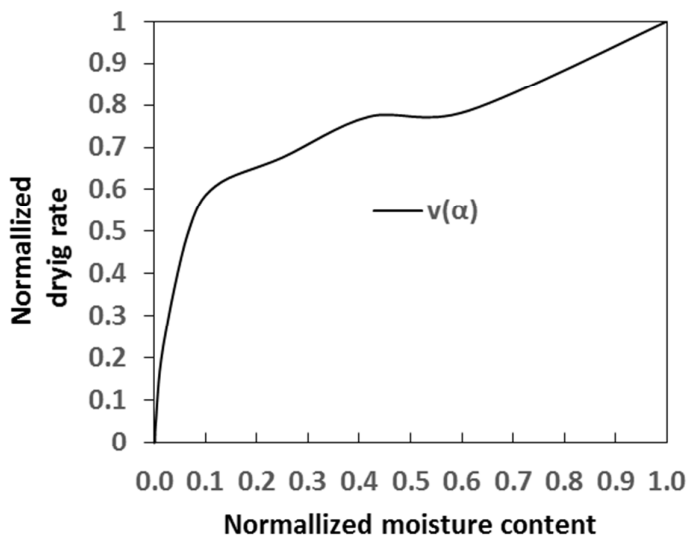
947

948

949

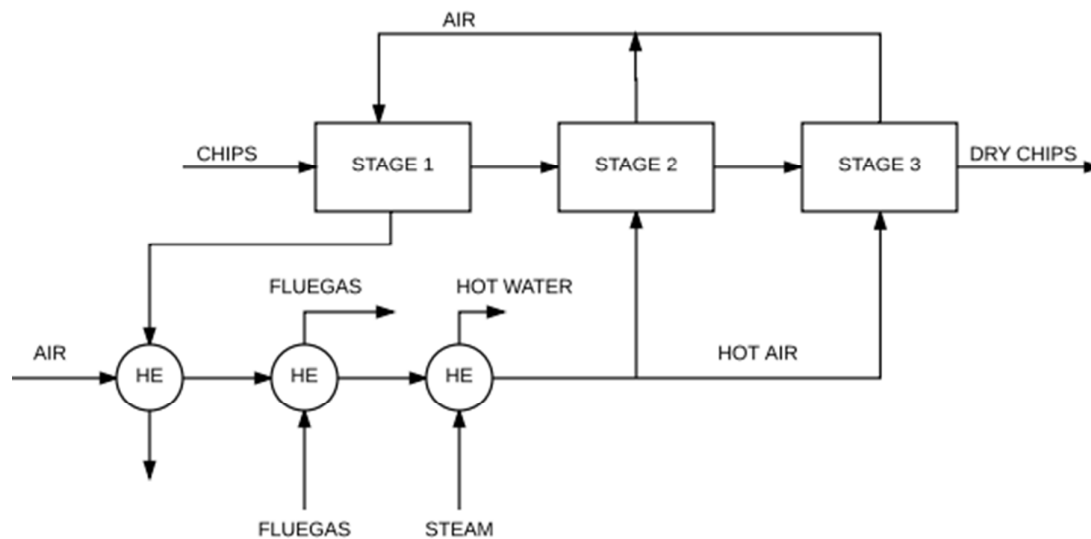
950

1
2
3 951
4
5 952
6
7
8
9
10
11
12
13
14
15
16
17
18
19
20
21
22
23
24
25
26



27
28
29
30
31
32
33
34
35
36
37
38
39
40
41
42
43
44
45
46
47
48
49
50
51 957
52
53
54
55
56
57
58
59
60

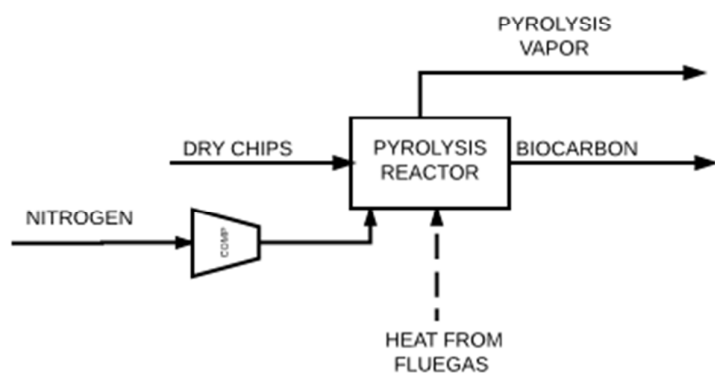
953
954 **Figure 3.** Normalized drying curve implemented in Aspen Plus model



51 957
52
53
54
55
56
57
58
59
60

958 **Figure 4.** Staged drying model in Aspen Plus

1
2
3 959
4
5
6
7
8
9



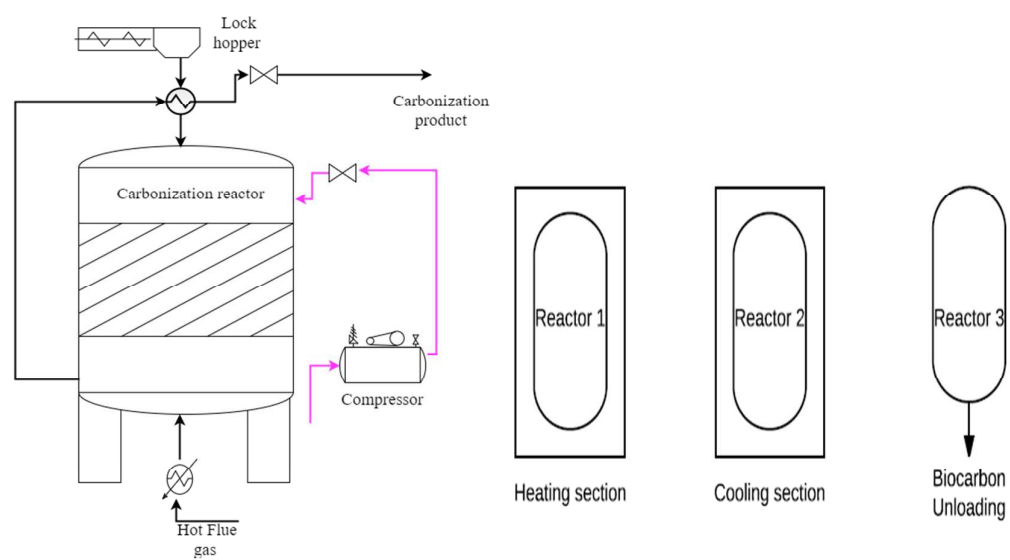
10
11
12
13
14
15
16
17
18

19 960
20
21

22 961
23 962

Figure 5. Simplified pyrolysis process flow diagram used in Aspen Plus

24
25
26
27
28
29
30
31
32
33
34
35
36
37
38
39
40
41

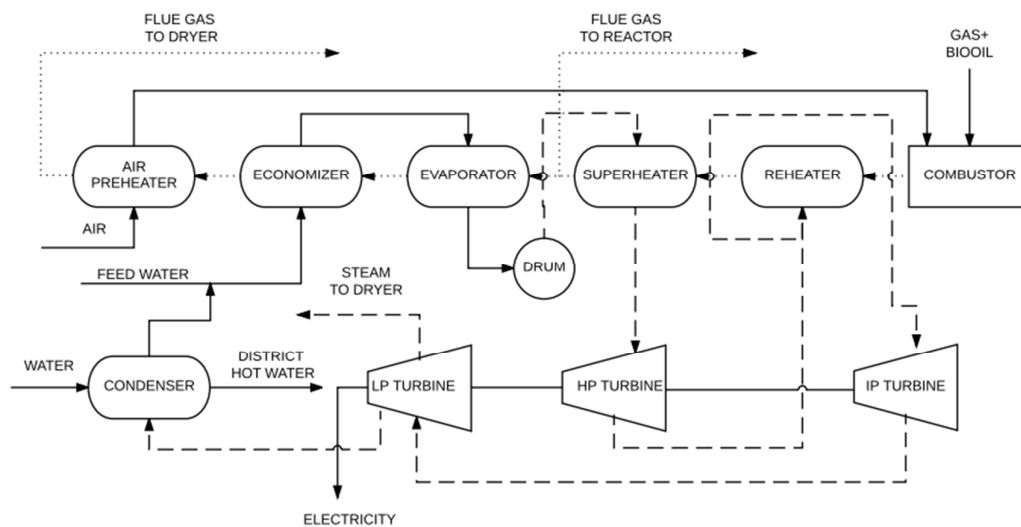


42 963
43 964

44 (a) (b)
45

46 965
47 966
48
49 967
50
51 968
52
53 969
54
55
56
57
58
59
60

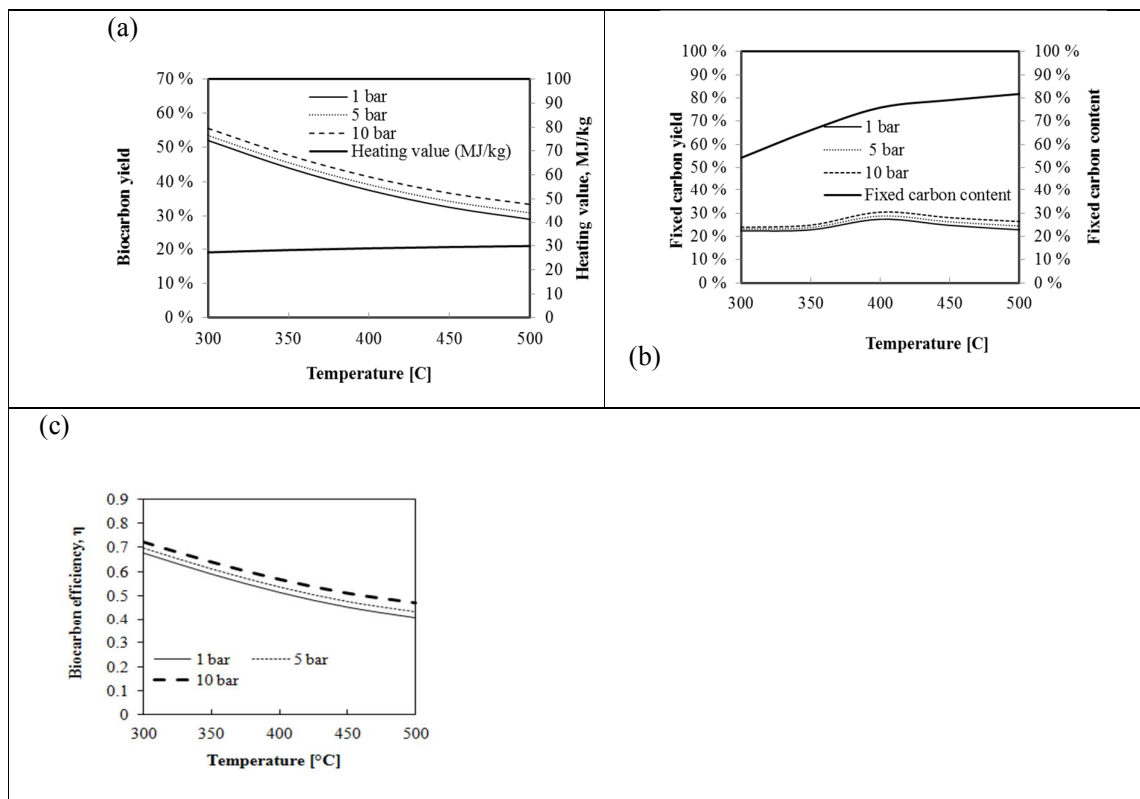
Figure 6. Pyrolysis reactor (a) and schematic idea of reactor in semi-continuous operating configuration (b) - modified Antal design³⁰



970

971 **Figure 7.** CHP process flow diagram

972



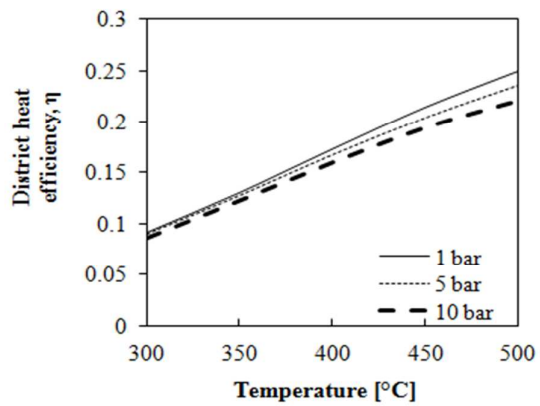
973 **Figure 8.** (a) Calculated biocarbon yield, (b) Fixed carbon yield, (c) Biocarbon energy

974 efficiency

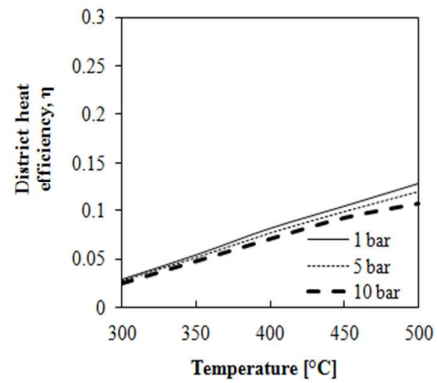
975

976

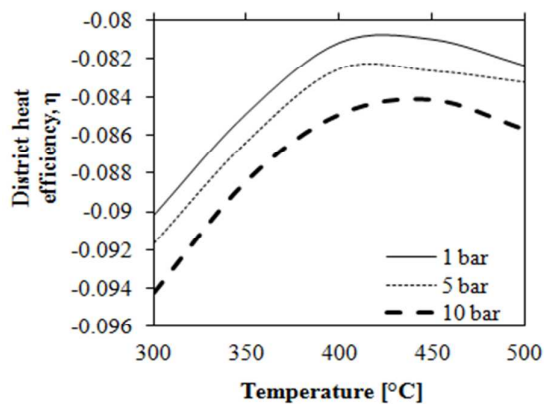
1
2
3 977
4
5 978
6
7 979
8
9 980
10
11
12 981
13
14 982
15
16
17
18
19
20
21
22
23
24
25
26
27
28
29
30
31
32
33
34
35
36
37
38
39
40
41
42
43
44
45
46
47
48
49
50
51
52
53
54
55
56
57
58
59
60



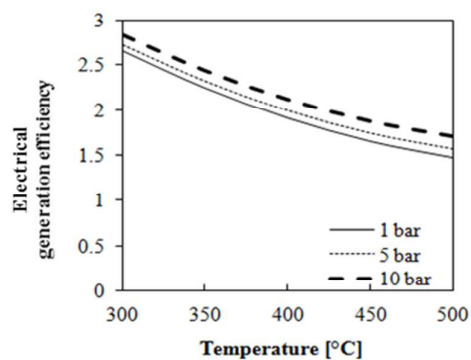
(a)



(b)



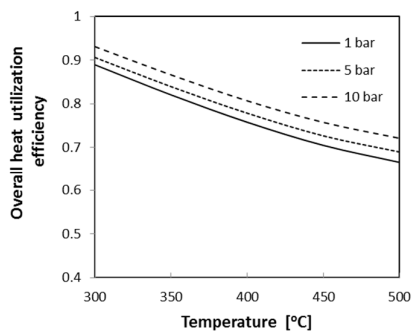
(c)



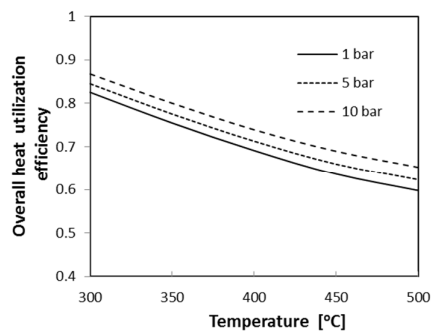
(d)

983 **Figure 9.** Effect of moisture content (wet basis) on district heat efficiency (a) 20%, (b) 40%, (c)
984 60% and electricity generation efficiency (d)

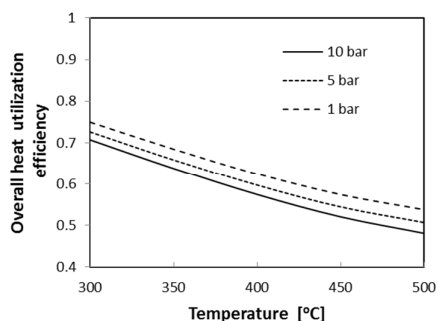
(a)



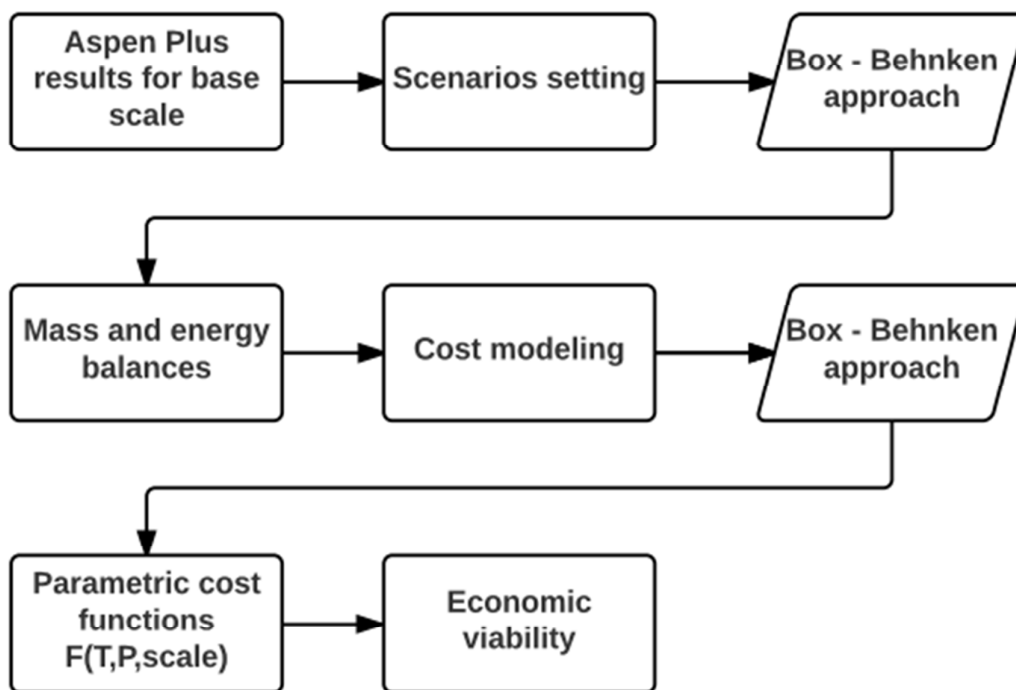
(b)



(c)

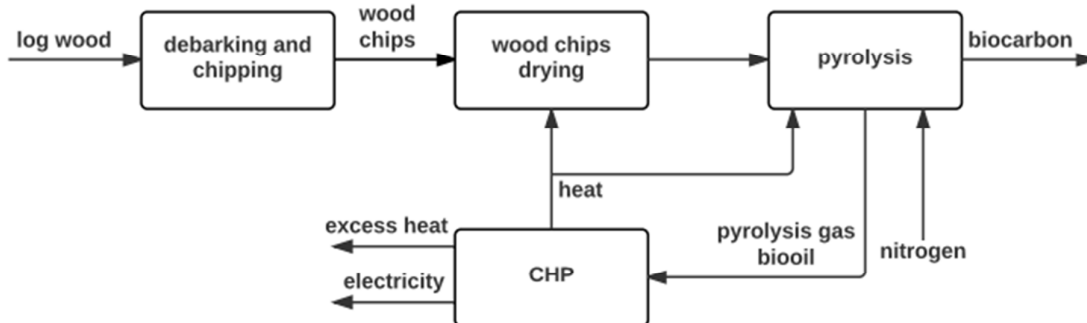


985 **Figure 10.** Overall heat utilization efficiency: (a) moisture content 20% wet basis, (b) 40%,
 986 (c) 60%



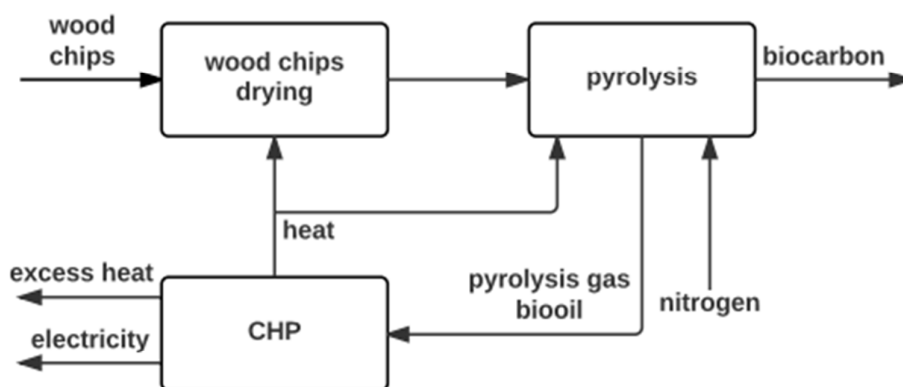
987
 988 **Figure 11.** The workflow of techno – economic analysis

989



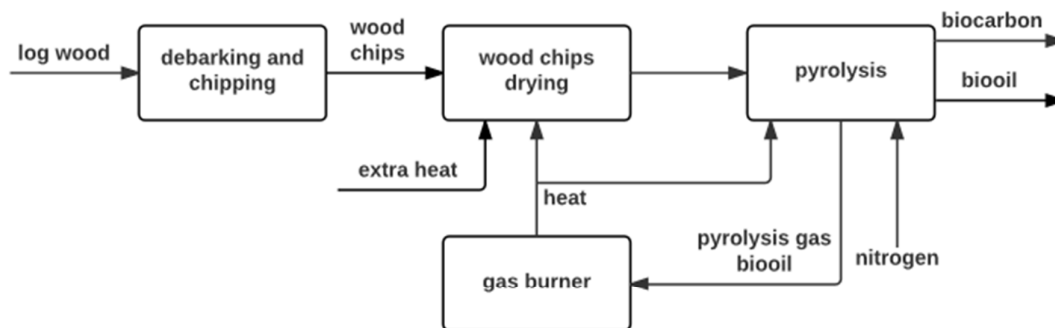
990

991 **Figure 12.** Simplified process flow diagram for Scenario A



992

993 **Figure 13.** Simplified process flow diagram for Scenario B



994

995 **Figure 14.** Simplified process flow diagram for Scenario C

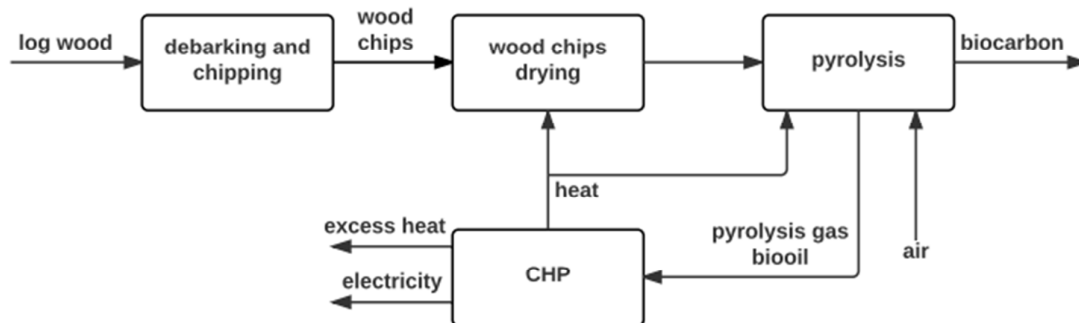


Figure 15. Simplified process flow diagram for Scenario D

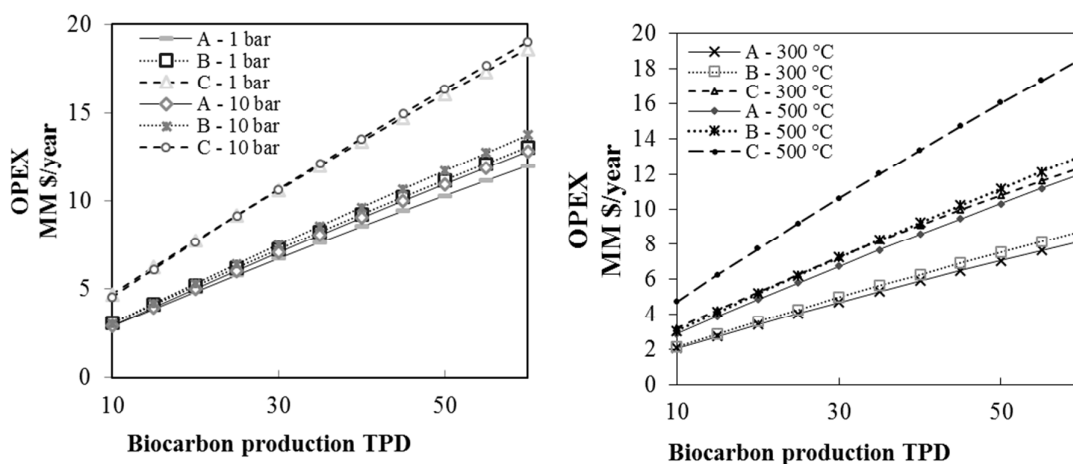


Figure 16. Influence of carbonization pressure (a) and temperature (b) on the OPEX for scenario A, B and C

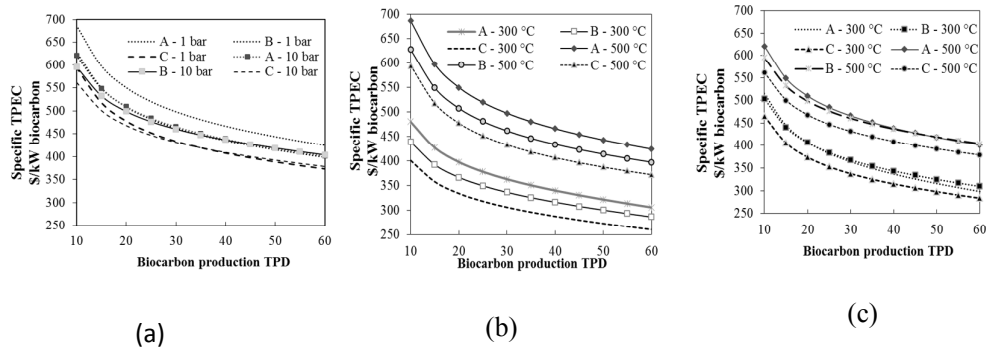


Figure 17. Influence of carbonization pressure (a) and temperature (b)-1 bar and (c)-10 bar on specific total purchase equipment cost (TPEC) for scenario A, B and C

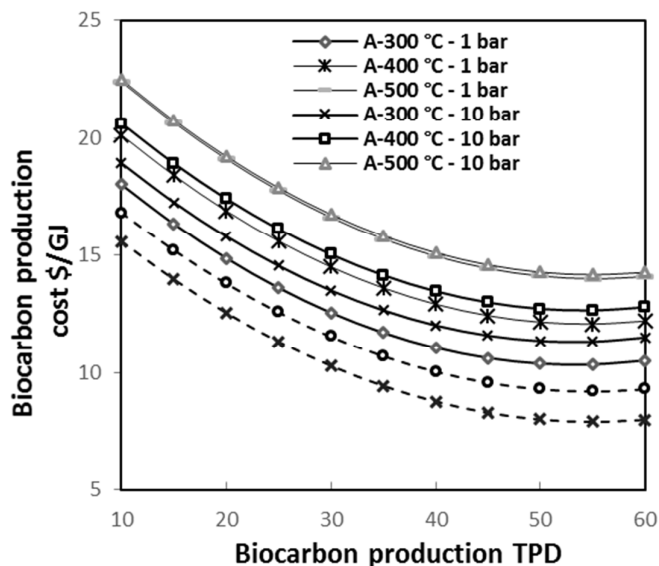
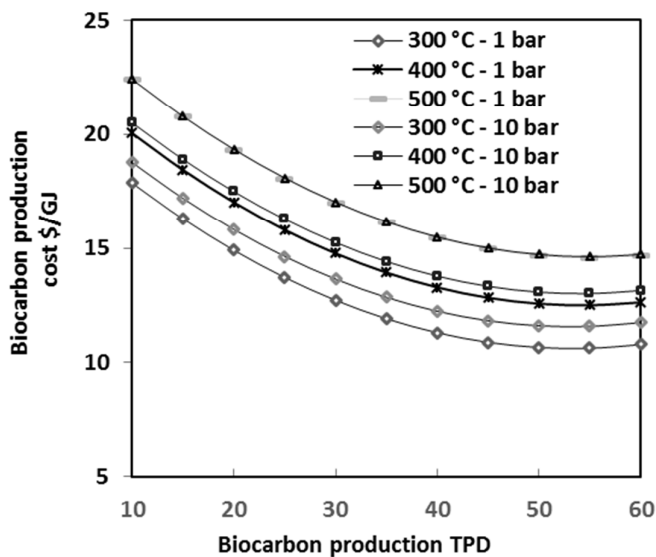
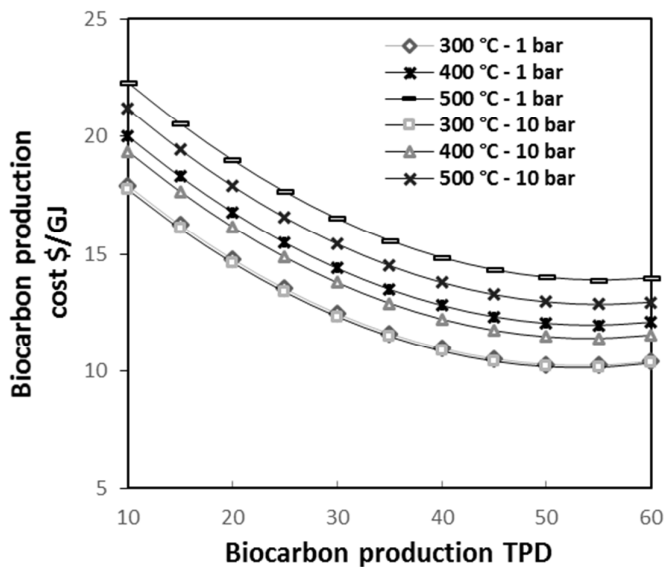


Figure 18. Influence of carbonization pressure and temperature for scenario A logwood conversion to biocarbon and Scenario C logwood conversion to biocarbon and biooil



1018

1019 **Figure 19.** Influence of carbonization pressure and temperature for scenario B woodchips
 1020 conversion to biocarbon



1021

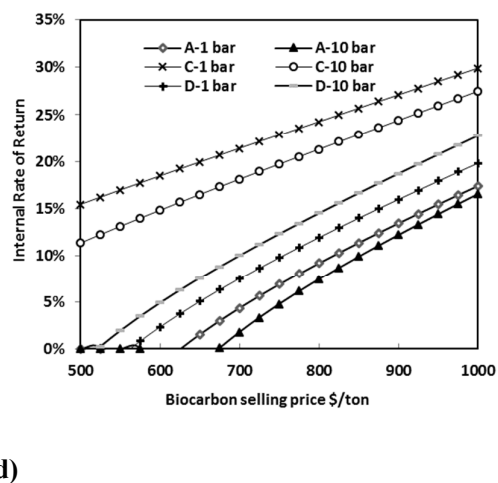
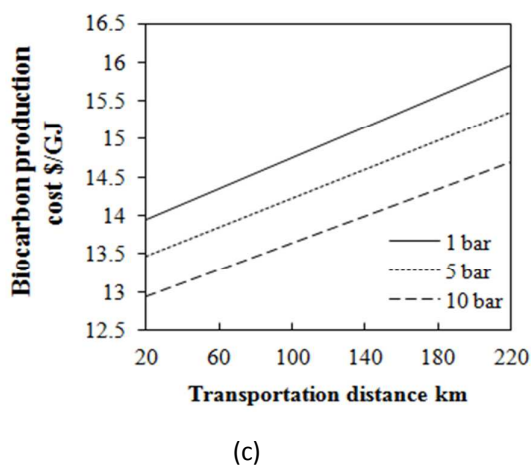
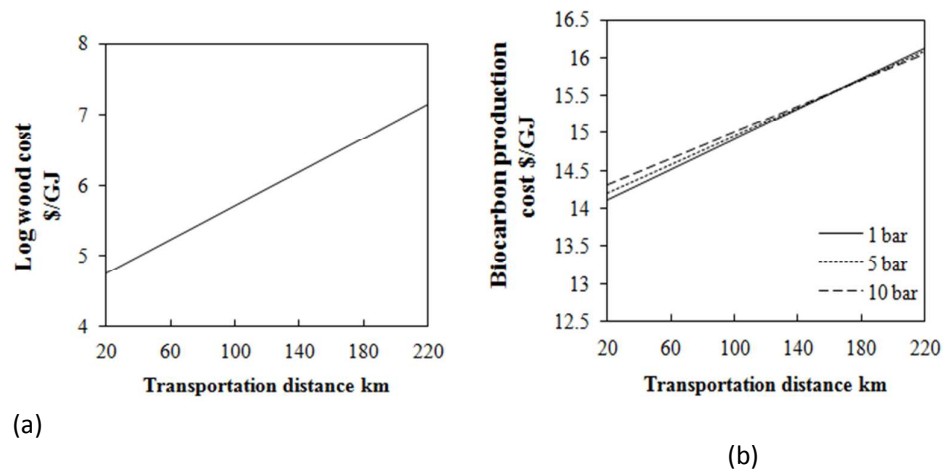
1022 **Figure 20.** Influence of replacing inert agent from nitrogen to air for scenario D for
 1023 logwood conversion to biocarbon

1024

1025

1026

1027



1028

1029 **Figure 21.** Influence of biomass transportation distance on (a) logwood cost, (b) biocarbon
 1030 production cost for case A – nitrogen as pressurized gas, (c) biocarbon production cost for
 1031 case D – air as pressurized gas and (d) internal rate of return versus biocarbon selling price
 1032 for case A, C and D

1033

1034

1035

1036

1037

1038

1039

1040 **List of Tables**1041 **Table 1.** Feedstock characteristics (Proximate and ultimate analysis, heating value)

Input fuel	Spruce stem wood	Spruce wood chips	Spruce bark	Spruce forest residues
Fixed carbon (% wt. dry)	27.27	19.65	26.85	24.49
Volatiles (% wt. dry)	72.43	79.97	70.62	69.82
Ash (% wt. dry)	0.30	0.38	2.53	5.69
C (% wt. dry ash free)	47.38	48.78	49.09	51.53
H (% wt. dry ash free)	6.40	6.27	6.06	6.51
O (% wt. dry ash free)	46.1	44.8	44.4	41.5
N (% wt. dry ash free)	0.09	0.13	0.45	0.44
S (% wt. dry ash free)	0.01	0.01	0.02	0.02
Cl (% wt. dry ash free)	0.002	-	0.04	0.02
HHV (MJ/kg dry)	19.90	20.13	20.25	19.94

1042

1043 **Table 2.** Woodchips size distribution

Size distribution (mm)	Weight fraction
63 – 45	0.04
45 – 31.5	0.08
31.5 – 16	0.69
16 – 8	0.06
8 – 3.15	0.09
3.15 – 0	0.03

1044

1045

1046

1047

1048

1049

1050

1051

1052 **Table 3.** Mass balance distribution (kg/kg dry ash free biomass) for 500 °C at different pressures

	Pressure [bar]					
	1	4	8	12	16	20
CHAR	0.30968	0.32469	0.34525	0.36642	0.38820	0.41059
BIOOIL (tar + water)	0.58667	0.57541	0.56000	0.54413	0.52780	0.51101
Tar	0.36039	0.34069	0.31372	0.28594	0.25735	0.22797
Phenol	0.18020	0.17035	0.15686	0.14297	0.12868	0.11398
Acetic acid	0.18020	0.17035	0.15686	0.14297	0.12868	0.11398
Water	0.22627	0.23472	0.24629	0.25819	0.27045	0.28305
GAS	0.11028	0.10647	0.10124	0.09586	0.09033	0.08463
H ₂	0.00036	0.00036	0.00036	0.00036	0.00036	0.00036
CH ₄	0.00727	0.00727	0.00727	0.00727	0.00727	0.00727
C ₂ H ₄	0.00001	0.00001	0.00001	0.00001	0.00001	0.00001
CO	0.05131	0.05131	0.05131	0.05131	0.05131	0.05131
CO ₂	0.05133	0.04752	0.04229	0.03691	0.03138	0.02568
TOTAL (CHAR+BIOOIL+GAS)	1.00663	1.00657	1.00649	1.00641	1.00632	1.00624

1053

1054

1055 **Table 4.** Specification of process design parameters used in the analysis

Process parameter	Value
Biocarbon output	10 ton/day
Raw logwood moisture (wet state)	20 – 60%
Bark content (weight fraction)	8%
Air temperature to the dryer	170 °C
Air pressure to the dryer	2 bar
Chips moisture content after dryer (wet state)	10%
Pyrolysis temperature	300 – 500 °C
Pyrolysis pressure	1 – 10 bar
SH steam temperature	550 °C
SH steam pressure	60 bar
IP steam temperature	550 °C
IP steam pressure	20 bar
LP steam temperature	220 °C
LP steam pressure	4 bar
Condensate temperature	80 °C
Feed water temperature after economizer	145 °C
Flue gas to stack temperature	120 °C

1056

1057

1058

1059

1060

1061

1
2
3 1062
4
5 1063
6
7
8
9
10
11
12
13 1064
14
15 1065
16
17 1066
18
19 1067
20
21 1068
22
23 1069
24
25 1070
26
27 1071
28
29 1072
30
31 1073
32
33 1074
34
35 1075
36
37 1076
38
39 1077
40
41 1078
42
43 1079
44
45 1080
46
47 1081
48
49 1082
50
51 1083
52
53 1084
54
55 1085
56
57 1086
58
59 1087
60 1088

Table 5. Overview of the different scenarios

Scenario	Feedstock	Pressurized gas	Electricity production	Products	
A	Logwood	Nitrogen	Yes	Biocarbon	-
B	Woodchips	Nitrogen	Yes	Biocarbon	-
C	Logwood	Nitrogen	No	Biocarbon	Biooil
D	Logwood	Air	Yes	Biocarbon	-

1089 **Table 6.** Biocarbon process equipments for the base scale scenario A (10 ton/day, 500 °C, 10 bar)

Equipment	Scale specification	Base scale S_b	Actual scale S	Max load/train	C_{S_b, I_b} MM\$	I/I_b	g	$f_{overall}$	$TPEC_i$ MMS	$C_{S, I, i}$ MMS	Ref
Logwood Storage	Mass, ton	33.5	2.26	110	1.000	1.457	0.6	2.34	0.174	0.591	⁴⁰
Debarking And Chipping With Auxiliary Equipment	Mass flow rate, ton/day	36.0	2.08	85	1.008	1.457	0.6	2.34	0.182	0.621	⁴⁰
DRYER - 3 Stages Belt	surface area, m ²	-	-	-	-	1.457	-	2.56	0.604	2.250	⁴¹
Dry Woodchips Storage	Mass flow rate, ton/day	33.5	1.33	110	1.000	1.457	0.6	2.34	0.123	0.418	⁴⁰
Chips Conveyor	Mass flow rate, ton/day	33.5	1.33	110	0.350	1.457	0.8	2.37	0.027	0.091	⁴⁰
Pyrolysis Reactor	Weight of the vessel, kg	-	-	-	-	1.946	-	4.14	0.452	3.642	³⁸
Compressor	Power, MW	10	0.015	-	6.030	1.457	0.6	2.51	0.076	0.278	⁴⁰
Biocarbon Conveyor	Mass flow rate, ton/day	33.5	0.42	110	0.350	1.457	0.8	2.37	0.010	0.036	⁴⁰
Biocarbon Storage	Mass, ton	33.5	0.42	110	1.000	1.457	0.6	2.34	0.058	0.197	⁴⁰
Steam Turbine And Steam System	MWe	10.3	0.13	-	5.100	1.457	0.7	2.37	0.236	0.815	⁴⁰
Burner	Volumetric flow rate m ³ /h	1.0	831.42	-	0.002	1.457	0.7	2.19	0.214	0.682	³⁷
Flue Gas Scrubber	Volumetric flow rate m ³ /s	10	1.94	64	0.053	1.457	0.5	2.50	0.023	0.085	³⁷
Bag Filter	Volumetric flow rate m ³ /s	1	1.94	-	0.005	1.474	1	2.50	0.009	0.034	³⁷
Total									2.188	9.741	

1090

1091

1092

1093

1094

1095

1096

1097

1098

1099

1100

1101

1102

1103 **Table 7.** Purchase equipment cost (TPEC, MMS) for the different scenarios (10 ton/day, 500 °C, 10 bar)

Equipment Name	Scenario A	Scenario B	Scenario C	Scenario D
Feedstock Storage	0.174	0.160	0.174	0.174
Debarking And Chipping With Auxiliary Equipment	0.182	0.000	0.182	0.182
Dryer - 3 Stages Belt	0.604	0.604	0.604	0.604
Dry Woodchips Storage	0.123	0.123	0.123	0.123
Chips Conveyor	0.027	0.027	0.027	0.027
Pyrolysis Reactor	0.452	0.452	0.452	0.452
Nitrogen Compressor	0.076	0.076	0.076	
Air compressor				0.070
Biocarbon Conveyor	0.010	0.010	0.010	0.010
Biocarbon Storage	0.058	0.058	0.058	0.058
Steam Turbine And Steam System	0.236	0.236	0.000	0.236
Burner	0.214	0.214	0.137	0.214
Flue Gas Scrubber	0.023	0.023	0.017	0.023
Bag Filter	0.009	0.009	0.005	0.009
Total Purchase Equipment Cost (TPEC)	2.188	1.992	1.865	2.188
Total Purchase and Installation Cost	9.741	9.073	8.639	9.741
Total Permanent Investment (TPI)	13.424	12.504	11.906	13.424

1104

1105

1106

1107

1108

1109

1110

1111

1112

1113

1114

1115

1116

1117

1
2
3 1118
4 1119
5 1120
6 1121
7 1122
8 1123
9 1124

Table 8. Cost associated factors to estimate the Total Permanent Investment (TPI) ³³

Factor	Cost associated factors	Typical value	Adopted value
f_{site}	Site preparation	0.05 – 0.2	0.05
f_{building}	Buildings	0.05 – 0.1	0.05
f_{land}	Land	0.05 – 0.1	0.05
f_{cont}	Cost of contingency	0.05 – 0.15	0.05
f_{eng}	Engineering	0.02 – 0.05	0.02
f_{dev}	Project development and	0.02 – 0.03	0.02
f_{com}	Commissioning	0.1	0.1

10
11
12
13
14
15
16
17
18
19 1125

20
21 1126

22
23 1127 **Table 9.** Labor cost for base scale plant of 10 ton/day biocarbon production

Position	Employed people, $E_{\text{ppl},i}$	Salary \$/year, D_i	Scaling factor, b_i
Plant Manager	1	120000	0
Plant Engineer	1	96000	0.6
Maintenance Support	1	72000	0.6
Lab Manager	1	72000	0
Shift Supervisor	1	72000	0.6
Lab Technician	1	72000	0.6
Maintenance Tech	1	72000	0.6
Shift Operators	4	72000	0.6
Yard Employees	1	60000	0.6
Clerks & Secretaries	1	72000	0.2
Total labor cost		\$996 000	

24
25
26
27
28
29
30
31
32
33
34
35
36
37
38 1128

39
40 1129

41
42 1130

43
44 1131 **Table 10.** Indirect operational costs $C_{\text{op},i}$

Indirect (Fixed) Operational Cost	Reference value
Maintenance, C_{maint}	2% C_{TPI}
Administration, C_{adm}	2% C_{TPI}
Insurance, C_{insur}	1% C_{TPI}

45
46
47
48
49
50
51
52
53
54 1132

55
56 1133

57
58 1134

59
60 58

1135 **Table 11.** Annual OPEX for different scenarios (10 ton/day, 500 °C, 10 bar)

Parameter	Scenario A	Scenario B	Scenario C	Scenario D
Biomass Supply	926 558	1 099 583	926 558	926 558
Fresh Water	593	593	432	593
Waste Water Treatment	10 159	10 159	7 411	10 159
Fly Ash Disposal	495	495	261	495
Nitrogen	333 793	333 793	333 793	-
Electricity	-	-	46 923	-
Heat	-	-	248 273	-
Labor cost	996 000	996 000	996 000	996 000
Maintenance	268 479	250 079	238 128	268 468
Administration	268 479	250 079	238 128	268 468
Insurance	134 240	125 039	119 064	134 234
Total, \$/year	2 938 796	3 065 819	3 154 971	2 604 974

1136

1137

1138 **Table 12.** Biomass supply variables under Norwegian conditions

Parameter	Value
Biomass density	500 kg/m ³
Forest exploitation cost	200 NOK/m ³
Cost of chipping (if buying chips)	48.4 NOK/m ³
Fixed transport cost	24 NOK/m ³
Variable transport cost	0.6 NOK/m ³ /km
Annual biomass production	1000 ton/km ²
1 NOK in USD	0.12 USD/NOK

1139

1140

1141 **Table 13.** Coefficients for biomass cost supply calculation

Coefficient	A – logwood	B – woodchips
X ₀	-325331	-400648
X _T	657	847
X _P	777531	913153
X _W	-4992	-4987
X _{TT}	0.34	0.35
X _{PP}	31453	36902
X _{WW}	34.1	33.4
X _{TP}	-2015	-2369
X _{TW}	223.74	262.85
X _{PW}	-10206	-11984

1142

1143

1144

1145

1146

1147

1148 **Table 14.** Financial parameters for biocarbon plant construction

1149

Financial parameter	Values/assumptions
Debt equity ratio	70-30
Depreciation model	Straight line depreciation model, depreciation period 20 years
Construction and commissioning duration	3 years period
% required capital during construction and commissioning	30% year 1, 40% year 2 and 30% year 3
Income tax rate	28%
Loan repayment period	10 years
Interest rate	7%
Currency and reference year	US\$ (2015)
Plant cost update	CEPCI 2015

1150

1151

1152

1153 **Table 15.** Direct variable operational costs and reference values for operational income³³

Parameter	Value
Fresh water	0.4865 \$/m ³
Waste water	8.34 \$/m ³
Fly Ash disposal	40 \$/ton
Nitrogen	0.353 \$/Nm ³
Electricity (scenario C)	0.111 \$/kWh
Heat (scenario C)	70 \$/MWh
Heat price	70 \$/MW
Electricity price	0.111 \$/kWh
CO ₂ intensity (Norway crude oil)	6.2 gCO ₂ /MJ
CO ₂ avoided emission	70 \$/ton
Biooil price	500 \$/ton

1154

1155